TÉCNICO LISBOA

Advanced Wind Farm Operation and Maintenance Strategies Considering Turbine Interaction

Chiara Bussolati

Thesis to obtain the Master of Science Degree in

Energy Engineering and Management

Supervisors: Prof. Ricardo Balbino Santos Pereira
Eng. Francisco Correia da Fonseca

Examination Committee

Chairperson: Prof. Edgar Caetano Fernandes
Supervisor: Prof. Ricardo Balbino Santos Pereira
Member of Committee: Prof. José Maria Campos da Silva André

October 2023

Declaration

I declare that this document is an original work of my own authorship and that it fulfils all the requirements of the Code of Conduct and Good Practices of the Universidade de Lisboa.

Abstract

The importance of offshore wind energy is increasing significantly, and more Countries are developing an interest in an offshore wind strategy. Nevertheless, there are locations where it is not possible to fix wind turbines to the seabed, due to the depth: in these areas, the structures that support the turbines must be floating. Among these location, Southern European countries, like Portugal, are investing in the offshore wind sector, to be able to build floating wind farms. The rise of new technologies also creates new challenges that must be faced: among them, maintenance is a critical aspect, as operations and maintenance account for 23 % of the overall costs of the project. As currently existing software and tools are mostly not opensource, it is of paramount importance to develop an algorithm that is able to reduce the costs associated with maintenance and, possibly, increase the annual energy production, to further decrease the levelized cost of energy.

The present thesis, developed in collaboration with WavEC, aims to plan preventive maintenance to meet these needs. To do so, the WindFloat Atlantic site in Viana do Castelo is chosen, as WavEC has extensive weather data and expertise in said location. The present work investigates the advantages given by optimizing the maintenance strategy considering wake effect, as opposed to a sequential scheduling.

Technical limitations of crew transfer vessels impose to only carry out maintenance activities under certain wind and sea conditions. As the most common vessels can only operate with relatively low significant wave height, novel vessels that are already on the market, although they are not as commonly used, have been considered. This allowed to broaden the workable windows significantly, and thus schedule preventive maintenance under favorable wind conditions. Namely, it is convenient to carry out maintenance when the wind speed is low, to reduce the downtime energy losses associated with it.

Several cases were simulated, changing four variables: vessel type (regular and novel), scheduling logic (optimized, sequential, and worst-case), criterium (binary and non-binary) and size of set of turbines (five and six, as novel crew transfer vessels can accommodate more crew member, hence being able to maintain more turbines in a single shift. The results obtained are very promising, as it was possible to significantly decrease downtime losses by implementing a non-binary criterium for preventive maintenance scheduling.

Keywords: Offshore wind energy, preventive maintenance, wake effect.

Resumo

A importância da energia eólica offshore está a aumentar significativamente, e cada vez mais países estão a desenvolver um interesse numa estratégia eólica offshore. No entanto, há locais onde não é possível fixar turbinas eólicas ao fundo do mar, devido à profundidade: nestas áreas, as estruturas que suportam as turbinas têm de ser flutuantes. Entre estes locais, países do sul da Europa, como Portugal, estão a investir no sector eólico offshore, para poderem construir parques eólicos flutuantes. O surgimento de novas tecnologias também cria novos desafios que têm de ser enfrentados: entre eles, a manutenção é um aspeto crítico, uma vez que as operações e a manutenção representam 23% dos custos globais do projeto. Como o software e as ferramentas atualmente existentes não estão, na sua maioria, disponíveis ao público, é de extrema importância desenvolver um algoritmo capaz de reduzir os custos associados à manutenção e, possivelmente, aumentar a produção anual de energia, para diminuir ainda mais o custo nivelado da energia. A presente tese, desenvolvida em colaboração com o WavEC, tem como objetivo planear a manutenção preventiva para responder a estas necessidades. Para o efeito, foi escolhido a localização do WindFloat Atlantic, em Viana do Castelo, uma vez que o WavEC dispõe de um histórico de dados meteorológicos e de experiência concreta nesse local. O presente trabalho investiga as vantagens de otimizar a estratégia de manutenção considerando o efeito de esteira, por oposição a uma calendarização sequencial. As limitações técnicas das embarcações de transferência de tripulação impõem que as actividades de manutenção só sejam efectuadas em determinadas condições de vento e mar. Uma vez que as embarcações mais comuns só podem operar com uma altura de onda significativa relativamente baixa, foram consideradas novas embarcações que já se encontram no mercado, embora não sejam tão utilizadas. Isto permitiu alargar significativamente as janelas de trabalho e, assim, programar a manutenção preventiva em condições de vento favoráveis. Nomeadamente, é conveniente efetuar a manutenção quando a velocidade do vento é baixa, para reduzir as perdas energéticas associadas ao tempo de paragem. Foram simulados vários casos, alterando quatro variáveis: tipo de embarcação (regular e nova), lógica de calendarização (optimizada, sequencial e de pior caso), critério (binário e não binário) e dimensão do conjunto de turbinas (cinco e seis, uma vez que as embarcações de transferência de tripulação novas podem acomodar mais tripulantes, podendo assim manter mais turbinas num único turno). Os resultados obtidos são promissores, uma vez que foi possível diminuir significativamente as perdas por inatividade através da implementação de um critério não binário para a calendarização da manutenção preventiva. Palavras-chave: Energia eólica offshore, manutenção preventiva, efeito de esteira.

Palavras-chave: Energia eólica offshore, manutenção preventiva, efeito esteira.

Acknowledgements

This Master Thesis was developed within the scope of the european research project 'ILIAD: INTEGRATED DigitaL Twins FOR MARINE AND MARITIME DATA AND INFORMATION SERVICES', with grant agreement number 101037643. Therefore, firstly, I would like to express my gratitude to WavEC, and especially to my supervisors Ricardo and Francisco, for involving me in this project and giving me the opportunity to participate in an important challenge for the offshore wind industry. Thank you for your constant feedback and for your advices, which have been very important during these months, and I am sure I will carry with me in my professional life.

There are many people I owe a big “thank you”, because I would not have been able to embrace this challenge without their constant support. The last two years have been a rollercoaster, and I value your support deeply.

My family, who always supported me, and never failed to show me how proud they are of me. You set a great example of effort and hard work for me that I tried to follow. Your unconditional love and pride have been, and will continue to be, my pillar: you make me believe in myself more and in my potential more than anyone else.

My friends, who always have my back: Daniela, Chiara, Chiara (another one), Francesco, Alice, Jacopo, Michela, Alberto, Giulia, Sara. You have no idea how important it was for me to know that, whatever happened, you were always there for me. I miss being able to see you every day, but I never felt left aside by you during these years. I knew I could always count on you, and that is what kept me striving. I hope you know how important you are to me.

The amazing people that I met in the past two years: Jake, Helena, Samir, Mariola, Jenn, Jaime, Floris, Juan, Mary, and many more – I would need another 60 pages to write all your names. I learnt so much from you, and you made these years the journey of a lifetime. This experience was new for all of us, and we supported each other through it – and had a lot of fun along the way. I met people that I hope will be in my life forever. Wherever life takes us, I will never forget you.

Table of Contents

List of Figures

List of Tables

Nomenclature

Acronyms and Abbreviations

AEP	Annual Energy Production
CTV	Crew Transfer Vessel
FLORIS	FLOw Redirection and Induction in Steady State
FOW	Floating Offshore Wind
FOWF	Floating Offshore Wind Farm
FOWT	Floating Offshore Wind Turbine
GFB	Gravity-Based Foundation
KPI	Key Performance Indicator
LCOE	Levelized Cost of Energy
NREL	National Renewable Energy Laboratory
O&M	Operations and Maintenance
OWF	Offshore Wind Farm
SCADA	Supervisory Control and Data Acquisition
Semi-Sub	Semisubmersible Platform
TLP	Tension Leg Platform

Latin Symbols

A	Swept area
a	Scale parameter
a	Induction factor
CF	Capacity Factor

C_p	Power coefficient
C_T	Thrust coefficient
$C(x)$	Maximum normalized velocity deficit
D	Rotor diameter
$E(T)$	Energy produced in timespan T
E_y	Yearly energy production
h	Height
h_{hub}	Hub height
H_s	Significant wave height
$H\ O\&M$	Hours of maintenance completed
I	Turbulence intensity
I_∞	Turbulence intensity (ambient conditions unperturbed by the turbine)
k	Shape parameter
k_t	Turbulence kinetic energy
$k_{t\infty}$	Turbulence kinetic energy (ambient conditions unperturbed by the turbine)
n	Turbines simultaneously maintained
P_{rated}	Rated power
P_t	Available power
$p(U)$	Weibull probability for wind speed U
r	Radial distance from center of the wake
T_C	Contingency time
T_L	Lead time

T_{POP}	Planned operation period
T_R	Reference period
U	Wind speed at rotor
U_h	Wind speed measured at height h
U_{hub}	Wind speed at hub height
U_w	Wind speed
U_{wlim}	Limit wind speed
U_∞	Wind speed at hub height
$v_{cut\text{-}in}$	Cut-in wind speed
$v_{cut\text{-}off}$	Cut-off wind speed
v_{rated}	Rated wind speed
x	Distance from upwind rotor
z_0	Surface roughness

Greek Symbols

α	Parameter that depends on the duration of the operation and the level of forecasting
ΔI	Added turbulence intensity
ΔI_m	Maximum added turbulence intensity
Δk_t	Added turbulence kinetic energy
$\Delta U/U\infty$	Normalized velocity deficit
$\delta(x)$	Wake width
$\mu_{0,}$	Statistical mode
ρ	Air density

σ	Standard deviation of the Gaussian-like velocity deficit profiles
$\sigma_{U\infty}$	Standard deviation of the wind velocity component in the average wind direction

1. Introduction

1.1 Motivation

As of 2022, the global Offshore Wind installed capacity sums up to 57.6 GW, and according to forecasts it will reach 519 GW installed by 2035 [1]. Nevertheless, currently offshore wind only makes up for 7% of the overall wind power installed, the remaining 93% being onshore. Even though the sector has grown significantly lately, decreasing the Levelized Cost of Energy (LCOE) of offshore wind energy down to 0.75 USD/kWh as of 2021 [2], the availability of offshore wind farms (OWFs) is only between 60 % and 70 %, whereas this number increases up to 95-99 % for onshore wind farms [3]. Among other reasons, OWFs require specialized operation and maintenance (O&M) activities, which are costly and complicated because of the harsh marine environment [2]. Operation and maintenance account for 23 % of the LCOE for an OWF, whereas this percentage is only 5 % for onshore wind farms. The main reason for this is the maintenance costs, namely the cost to replace the equipment and revenue losses due to downtime of the turbines, as well as vessels costs [4]. Therefore, the interventions must be planned meticulously to reduce the LCOE. This can be done in two ways: reducing the costs or improving the energy production. A well-planned O&M schedule can achieve both, hence further decrease the LCOE.

Optimization models must consider several factors, including weather conditions, vessel and personnel availability, downtime losses, and should consider different maintenance strategies. Different models have been developed, but most of them only optimize some aspects of the strategies, thus requiring the user to have knowledge about how maintenance can be improved. Ideally, a model should allow unexperienced users to extract information [5].

Currently existing decision-making tools can be differentiated according to:

- Decision-making timescale (long-term, based on historical data, or short-term, based on weather forecast);
- Project phase;
- Target sector;
- Licensing type;
- Software functionalities [6].

Most of the available tools for marine renewable energy projects are not open source, therefore lacking in transparency and improvements thanks to community collaborations. For this reason, it is of paramount importance for players in the industry to develop their own algorithm to optimize maintenance scheduling. Moreover, they do not allow vessel selection, which is a critical aspect since vessel hiring accounts for 73 % of the total O&M costs [6].

1.2 Objective

The present thesis builds up on previous works, to add detail to them, and aims to decrease the energy losses caused by downtime. Specifically, preventive maintenance is evaluated, with decision-making models not only to understand if it is possible to perform the maintenance intervention, but also whether it is convenient to do so or if it is better to adopt a more conservative strategy. In fact, the objective is not only to determine if an intervention is feasible but also if it is convenient, considering that the workable window for maintenance includes seven months, from April to October, and it is not ideal to end preventive maintenance too soon, since better weather conditions usually occur during summer months.

The objective of the present work is to assess the impact of considering aerodynamic interactions between turbines to schedule preventive maintenance, such that downtime energy losses are minimized, as opposed to performing maintenance in a sequential order. Namely, wake effects are analyzed, to discover if it is a key factor to consider to decide which turbines to maintain under certain wind conditions.

To do so, the open-source software Flow Redirection and Induction in Steady state (FLORIS) is used. FLORIS is a Python package that can be used to calculate the energy production of a given wind farm, considering wake losses, hence it is a suitable tool for the scope of the present work.

1.3 Thesis Outline

The present thesis explores possible strategies to reduce the LCOE of a floating offshore wind farm (FOWF), by optimizing the preventive maintenance strategies, and thus increasing the annual energy production of said farm.

Chapter 1 focuses on the importance of optimizing preventive maintenance for floating offshore wind (FOW), hence the motivations for the present work and its objective.

Chapter 2 covers the theory background. Firstly, the state of the art of wind turbines and foundations is presented, followed by an overview of existing OWFs. Then, theoretical concepts on the energy production model for wind turbines are explained; followed by the description of wake effect, its consequences on a wind farm's production and the models used to describe said effect. After this, FLORIS, a Python package that can be used to calculate a wind farm's energy production considering wake effect, is presented. Finally, maintenance strategies are addressed, describing the existing approaches and related terminology.

Chapter 3 describes the case study examined and the methodology followed to reduce the downtime energy losses in said case study. This section is organized atypically, as the Case Study is partially defined first. This is because the methodology used is closely related to the characteristics of the wind farm. Therefore, it is necessary

to define some of the characteristics of the wind farm to make decisions on certain aspects, as the details of the methodology depend on them.

Chapter 4 discusses the results obtained from the simulations conducted with FLORIS. All the cases are addressed, particularly in comparison to the Base Case, to evaluate the impact of the maintenance strategy developed on downtime energy losses and annual energy production (AEP).

Chapter 5 draws conclusions based on the previously described results, and hints at possible developments for future works to build up on the present thesis.

2. Theory Background

2.1 State of the Art

Offshore Wind Turbines and Foundations

Since the first OWF in Vindeby, turbine size grew significantly, in order to increase the swept area and the hub height, therefore producing more power with a single machine. Currently, the largest operational wind turbine is Vestas V236-15.0MW, with a nominal capacity of 15 MW and a 236 m rotor diameter, allowing for a capacity factor over 60 % [7]. As the turbine successfully produced its first kWh in Denmark, Vestas announced that it will be produced serially from late 2023 [8]. Further steps are being made by Chinese CSSC Haizhuang, as they are developing a 18 MW wind turbine, with a diameter of 260 meters [9]. Future turbines are expected to reach even bigger sizes, as projects are already being proposed with turbines up to 20 MW [10].

Along with the development of wind turbines, that of foundations is also extremely important for OWFs. Figure 2.1 shows the different types of foundations that are used for offshore wind turbines (OWTs), fixed and floating. Grounded systems can only be used for water depths up to 60 meters, whereas floating systems must be adopted for deeper waters, in locations like Southern Europe.

Among bottom-fixed systems, the most common are: Gravity-Based Foundations (GBFs), Monopile Foundations, Tripod Foundations and Jacket Foundations [11]:

- GBFs use cheap materials, such as concrete and steel for the structure, as well as gravel and sand for the ballast. It is a highly developed technology, as it is used in the oil and gas industry. On the other hand, it is only suitable for water depths up to 30 m and it can have negative environmental impacts.
- Monopile Foundations are convenient from a costs point of view for water depths up to 40 m. They are easy to install and adapt to various turbine sizes.
- Tripod Foundations are cost-effective for water depths up to 45 meters. The installation of these foundations is simple, as the seabed does not require any preparation.
- Jacket Foundations can exploit waters up to 60 meters deep and their considerable size can provide a new habitat for several species, without endangering them. Moreover, these foundations are economical due to the well-established construction methods, as they are similar to offshore oil platforms. On the other hand, they may favor the development of invasive species and endanger marine species due to noise [11].

Foundations are a very important component of an OWF, but fixing a turbine to the seabed is only feasible up to around 60 meters of depth. For deeper waters, floating foundations are more suitable, and they have already been used in waters as deep as 300 meters [12]. So far, four main types of floating systems have been developed:

Barge Platforms, Semisubmersible Platforms (Semi-sub), Spar-Type Platforms, and Tension Leg Platforms (TLPs) [13].

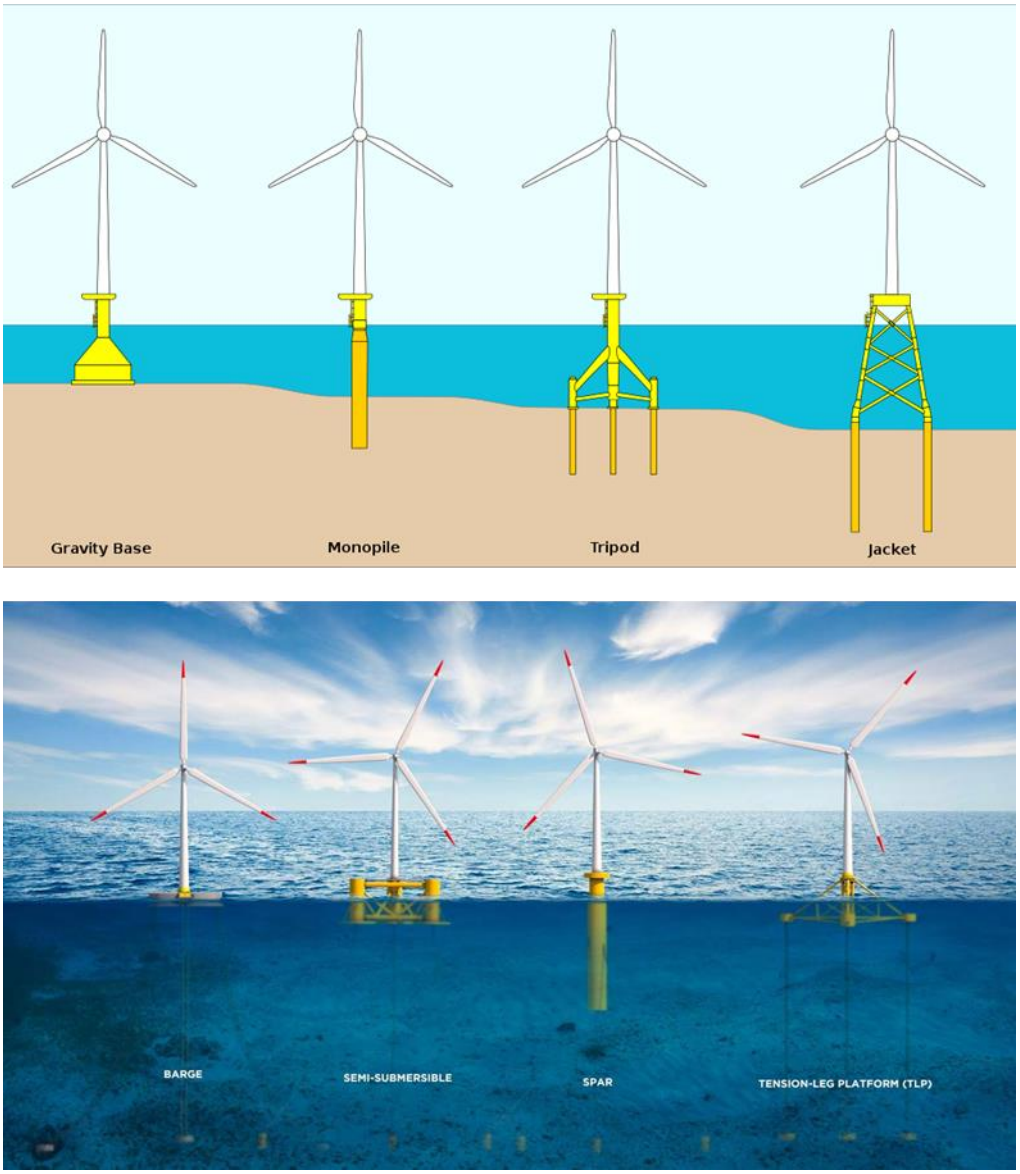

Figure 2.1 - Types of offshore wind foundations. [Above] Bottom-fixed, [Below] Floating. Retrieved from *[14]*, *[15]*

In the offshore wind sector, O&M accounts for 30% of the overall costs, hence reducing this cost is a key factor to make floating offshore wind economically competitive against bottom-fixed structures. In fact, floating foundations will require new solutions to overcome the impossibility to use conventional vessels in such deep waters [16]. Moreover, floating turbines are subject to more motions than bottom-fixed foundations, making the maintenance interventions more challenging for the former [16].

Existing Projects

The first OWF was built in Vindeby, Denmark in 1991 and commissioned by Ørsted. The plant consisted of 11 wind turbines with concrete foundations in shallow waters, for a total of 5 MW installed, meaning that each turbine had a nominal capacity around 0.4 MW. In the following ten years, the project was followed by other installations in Northern Europe: Denmark, the Netherlands, Sweden and United Kingdom, the projects' mean size being around 20 MW.

Later, new markets came into play, including Belgium, Germany, and Finland, as well as China. The market size grew from 250 MW to 6.4 GW between 2001 and 2012. The mean installed power for a plant grew by five times, reaching 100 MW and the LCOE started decreasing.

After 2012, the market size increased significantly and the LCOE decreased dramatically, making bottom-fixed offshore wind installations competitive with traditional energy sources and with other renewables [17]. Table 2.1 summarizes the global offshore wind capacity added each year starting from 2013. In 2022, the global installed capacity reached 57.6 GW, 44 % of which is installed in China. Overall, out of 257 OWFs, 140 are in Asia, 115 in Europe and 2 in the United States of America [1].

Table 2.1 - Annual added offshore wind capacity. Adapted from *[1]*

Year	2013	2014	2015	2016	2017	2018	2019	2020	2021	2022
Added Capacity [MW]	2,042	1,043	3,668	1,254	4,216	5,079	5,194	5,206	15,666	9,433

In Europe, most of the OWFs are installed in northern countries, because of the favorable wind conditions and because the shallow waters of the North Sea are particularly suitable for installing OWTs, as the average water depth is 90 m [18]. The country with the highest installed capacity is the United Kingdom (13.6 GW as of 2022), followed by Germany (8 GW), the Netherlands (3 GW), Denmark (2.34 GW), and Belgium (2.26 GW), which are the only European countries with at least 1 GW of offshore wind installed capacity. In 2022, the Saint Nazaire OWF was commissioned in France; with 480 MW of installed capacity, it is the first large scale offshore wind project of the Country. Moreover, Sweden and Finland have 191 MW and 71 MW of offshore wind installed capacity respectively [1]. In 2023, Norway completed the construction of the Hywind Tampen FOWF, the world's largest FOWF with a capacity equal to 88 MW, reaching a total of 96 MW of offshore wind power installed [19].

Unlike the North Sea, the Mediterranean Sea and the Southern Atlantic Ocean are characterized by deeper waters; hence, in most of the locations, floating foundations are required. Therefore, Southern European countries have not fully deployed the offshore wind technology yet: the country with the highest installed is Italy

with 30 MW, followed by Portugal (25 MW) [1]. The Beleolico wind farm in Italy comprises 10 turbines located just 100 m from the port of Taranto, and, thus, it is classified as a nearshore wind farm [20]. On the contrary, WindFloat Atlantic in Portugal is located 20 km far from the shore of Viana do Castelo, where the water depth reaches 100 m. Therefore, floating foundations are used to support the three turbines. WindFloat Atlantic is the first commercial scale project to use the semi-submersible technology [21], followed by the Kincardine OWF in Scotland [22].

The European FOWFs, currently operational and under construction, as of 2023, are listed in Table 2.2. As the demo projects resulted successful, France has already launched a 250 MW tender for FOWFs off the coast of Brittany and will soon launch two more tenders, 250 MW each, of floating projects in the Mediterranean. Spain, Portugal, and Norway are expected to follow this year, and Italy, Ireland and Greece are preparing to do the same [23]. This will furtherly increase the importance of offshore wind in Europe, thanks to floating technologies, which will allow to install turbines in deeper waters; hence unlocking several opportunities for Southern European countries especially.

Table 2.2 – FOWFs in Europe as of 2023 *[12], [21] , [22], [24], [25], [26], [27] , [28], [29], [30], [31]*

Farm	Country	Capacity	Platform	Status	Type
Hywind Tampen	Norway	88 MW	Spar-type	Operating	Commercial
Kincardine	UK	50 MW	Semi-Sub	Operating	Commercial
Hywind Scotland	UK	30 MW	Spar-type	Operating	Pre-Commercial
WindFloat Atlantic	Portugal	25 MW	Semi-Sub	Operating	Pre-Commercial
EFGL	France	30 MW	Semi-sub	Construction	Commercial
EolMed	France	30 MW	Barge	Construction	Pre-commercial
Provence Gran Large	France	24 MW	TLP	Construction	Pre-commercial
TetraSpar	Norway	3.6 MW	Spar-type	Operating	Demo
Floatgen	France	2 MW	Barge	Operating	Demo
DemoSATH	Spain	2 MW	Barge	Operating	Demo
X1Wind	Spain	0.2 MW	TLP	Operating	Demo

2.2 Energy Production Model

As one of the key performance indicators (KPIs) to evaluate the feasibility of an energy plant is the LCOE, it is of paramount importance to describe how the electricity production for a wind farm can be calculated, since increasing the latter is a way to decrease the LCOE. The total available power content of the wind flow can be calculated through Equation 2.1, where P_t is the available power, ρ is the air density, A is the swept area of the

turbine and *U* is the velocity of the wind flow investing the rotor. Nevertheless, it is impossible to extract all the available power: the actual power that is produced by a wind turbine invested by a wind flow is computed through Equation 2.2.

$$P_t = \frac{1}{2}\rho A U^3$$

Equation 2.1

$$P = C_p P_t = \frac{1}{2} C_p \rho A U^3$$

Equation 2.2

C_p is the power coefficient and it has a physical limit set by Betz's law equal to 59.3 % [32], although it is typically lower due to mechanical, electrical, and aerodynamic losses, as well as control strategies for power regulation. At full load, power regulation through control strategies is performed, to guarantee the quality of the electricity produced. To do so, C_p is lowered, as the risk of turbine failure would increase if the rotational velocity is too high. This is displayed in Figure 2.2, which shows the power curve and power coefficient curve for the IEA 15 MW Reference Turbine. In the power curve, three reference velocities can be identified:

- $v_{cut\text{-}in}$: wind speed at which the turbine starts producing power;
- v_{rated}: wind speed at which the wind turbine reaches its rated power production;
- $v_{cut\text{-}off}$: wind speed at which the turbine stops producing power.

Between $v_{cut\text{-}in}$ and v_{rated} there is the partial load region, which follows Equation 2.2. On the other hand, between v_{rated} and $v_{cut\text{-}off}$ there is the full load region, where pitch control is performed to limit the power output to the rated value, hence the power coefficient decreases. Finally, for wind speeds higher than the cut-off velocity, the turbine is shut off to avoid damage.

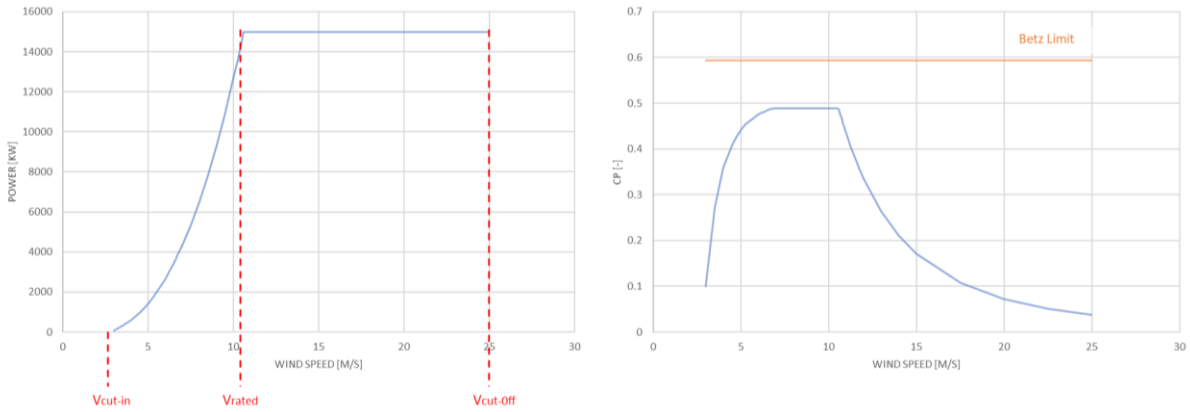

Figure 2.2 - Power Curve [Left] and Cp compared to Betz Limit [Right] for IEA 15 MW Reference Turbine. Data from *[33]*

The energy produced in a certain timespan can be calculated as the integral of the power over the said timespan, T:

$$E(T) = \int_0^T P(t)dt$$

Equation 2.3

If the turbine operates at constant rated power, P_{rated}, the energy produced can be calculated as the product of the rated power and the timespan. The ratio between the energy produced and the energy that would be produced if the turbine was operating constantly at rated power is called Capacity Factor (CF) and it is defined in Equation 2.4. This value varies significantly, and it typically ranges between 0.35 and 0.45 for OWFs, whereas it only reaches 0.30 for onshore wind farms.

$$CF = \frac{E}{E_{rated}} = \frac{1}{T}\int_0^T \frac{P(t)dt}{P_{rated}}$$

Equation 2.4

The use of these equations requires discrete measurements that can take a very long time; hence it is convenient to use statistical analysis. The Weibull distribution gives a good representation of the probability of different wind speeds to occur.

$$p(U) = \frac{kU^{k-1}}{a^k} e^{-\left(\frac{U}{a}\right)^2}$$

Equation 2.5

Where *k* is the shape parameter, typically equal to 2 for offshore sites, and a is the scale parameter.

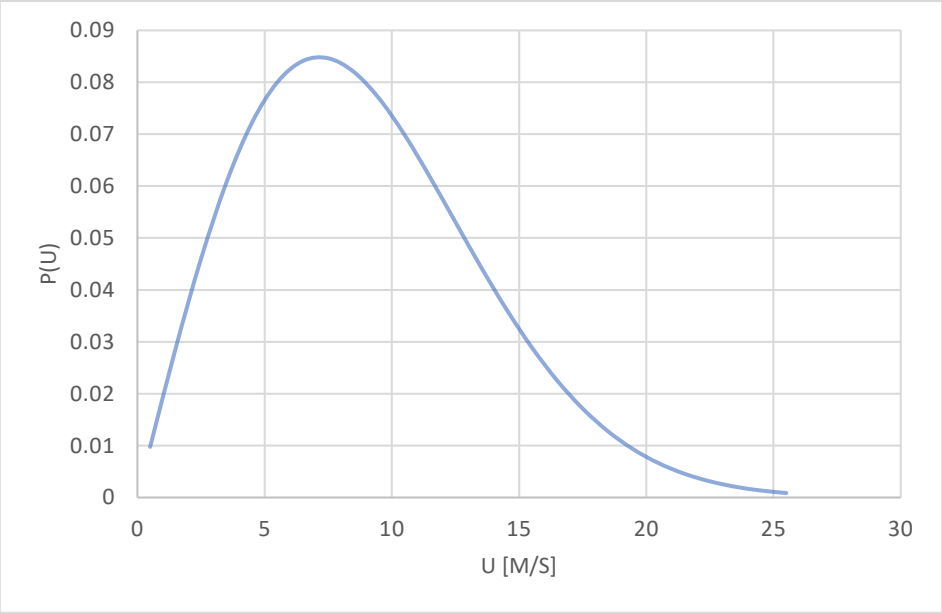

Figure 2.3 - Example of Weibull probability function

Hence, it can be assumed that for a certain time interval, *T*, equal to the product of *p(U)* and the hours in a year (8760), the power output is constant and Equation 2.3 can be rewritten as Equation 2.6 and the yearly energy production can be written as in Equation 2.7.

$$E_i = P_i T_i = P * p(U_i) * 8760$$

Equation 2.6

$$E_{yearly} = \sum_{i=1}^{N} P * p(U_i) * 8760$$

Equation 2.7

2.3 Wake Effect in Wind Farms

As a wind turbine converts the kinetic energy of the wind to electrical energy, the wind flow behind the rotor, which is called wake, is subject to a velocity deficit, according to the first principle of thermodynamics [34]. Hence, the wind flow investing another turbine, located behind the first, has a speed reduction around 15 – 20 % [35], resulting in an energy loss for the farm. Moreover, turbulences are created, increasing the mechanical loads on the downstream turbine [36]. The wake behind a turbine can be differentiated into near wake and far wake, where the velocity gradually increases back to its normal value [37]. This effect, called wake effect, is of paramount importance, especially now that the size of wind turbines is increasing, and farms are being designed with a higher number of turbines. Therefore, it is key to consider the interactions between turbines [37].

Several models have been developed to approximate this effect, in order to minimize the losses of a wind farm. Among the most widely used models, there is the Jensen model. Jensen's model uses mass conservation to derive an equation that calculates the velocity deficit as a function of the distance downstream [38]. The result is a top-hat model to describe the velocity deficit, which approximates the energy content rather than the velocity deficit itself [39]. This can lead to a lack of precision in approximating the velocity deficit as, according to Equation 2.1, a small mistake in the approximation of velocity can cause a relevant mistake when calculating the power production, especially due to said model's inaccuracy when calculating the power production of single wind turbines within the farm [40]. Hence, to add precision to the calculations, in the present work the Gaussian Model will be used.

Gaussian Model for Wake Velocity Deficit

The Gaussian Model for wake effect, proposed by Majid Bastankhah and Fernando Porté-Agel, is derived applying the conservation of mass and momentum and assuming a Gaussian distribution for the velocity decrease downstream [39]. It is a more advanced model than the widely used Jensen model, as the latter does not consider momentum conservation [35]. This model assumes a gaussian-shaped velocity deficit profile, which is compared to the top-hat shape in Figure 2.4. The shape of the velocity deficit profile obtained with Jensen's model has a discontinuity between the area within the rotor diameter and the area outside of it, which is not suitable to describe the real physical phenomenon.

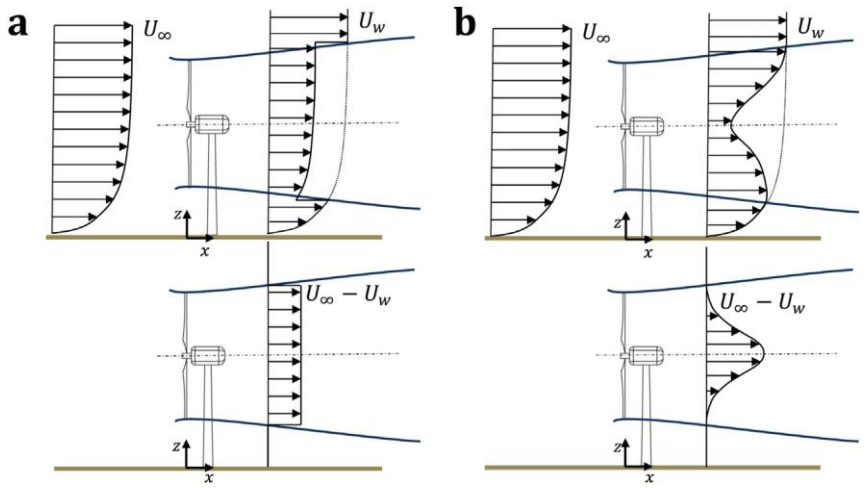

Figure 2.4 - Schematic of the vertical profiles of the mean velocity (top) and velocity deficit (bottom) downwind of a wind turbine obtained by assuming: (a) a top-hat and (b) a Gaussian. Retrieved from [39]

According to [39], the velocity deficit can be described with Equation 2.8 as the product of the maximum normalized velocity deficit at each downwind location occurring at the center of the wake and a function of the radial distance from the center of the wake and the wake width at each value of *x*, which is the distance from the upwind rotor.

$$\frac{\Delta U}{U_\infty} = C(x) f\left(\frac{r}{\delta(x)}\right)$$

Equation 2.8

As the latter is, as said, a gaussian distribution, and *C(x)* can be computed with Equation 2.9, the velocity deficit can be calculated as displayed by Equation *2.10* [41].

$$C(x) = \left(1 - \sqrt{1 - \frac{C_T}{8\left(\sigma/D\right)^2}}\right)$$

Equation 2.9

$$\frac{\Delta U}{U_\infty} = \left(1 - \sqrt{1 - \frac{C_T}{8\left(\sigma/D\right)^2}}\right) e^{\frac{-r^2}{2\sigma^2}}$$

Equation 2.10

Turbulence Intensity Wake Model

As mentioned above, turbulence is generated in the wake of a wind turbine, causing mechanical loads on the downstream wind turbine. According to Crespo and Hernandez [42], the turbulence intensity, *I*, is defined as the ratio between the standard deviation of the wind velocity component in the average wind direction and the wind velocity at hub height (Equation 2.11):

$$I_\infty = \frac{\sigma_{u\infty}}{U_\infty} = 1.026\frac{k_\infty^{0.5}}{U_\infty}$$

Equation 2.11

Where *k* is the turbulence kinetic energy. Therefore, the added turbulence intensity. As the turbine creates an additional turbulence kinetic energy in the wake, equal to Equation 2.12, the added turbulence intensity can be defined according to Equation 2.13.

$$\Delta k = k - k_\infty$$

Equation 2.12

$$\Delta I = (I^2 - I_\infty^2)^{0.5}$$

Equation 2.13

Given the general formulation, there is a differentiation to be made between the near wake and the far wake regions. In the near wake ($0.5 < D/H < 1$; $0.07 \leq I\infty < 0.014$; $0.2 < C_T < 0.96$), Equation 2.14 is valid to calculate the maximum turbulence intensity. On the other hand, in the far wake ($5 < x/D < 15$; $0.07 < I\infty < 0.014$; $0.1 < a < 0.4$), Equation 2.15 is used.

$$\Delta I_m = 0.725a = 0.362[1 - (1 - C_T)^{0.5}]$$

Equation 2.14

$$\Delta I_m = 0.73a^{0.8325}I_\infty^{0.0325}\left(\frac{x}{D}\right)^{-0.32}$$

Equation 2.15

As the far wake is the region where the velocity deficit effect decreases, Equation 2.16 is used in the present work, since the downstream turbine is in the far wake of the upstream one. For multiple wakes added turbulence intensity:

$$\Delta I = \sqrt{\sum_j \Delta I_j^2 + I_0^2}$$

Equation 2.16

Where ΔI_j is the added turbulence intensity on the downstream turbine due to the upstream turbine j and I_0 is the ambient turbulent intensity [42].

Katic Wake Combination Model

As a wind farm is considered, a turbine is not subject to the wake of just another turbine. Instead, it is invested by the wake of several turbines. Therefore, it is necessary to adopt a model to describe this event: the Katic model [43] is widely used for the purpose, and it states that the combined kinetic deficit of two or more wakes at a certain downwind position is calculated as the sum of the kinetic energy deficits of each wake. Therefore, U_i, the wind speed investing a certain turbine, i, can be calculated through Equation 2.17:

$$U_i = U_\infty - \sqrt{\sum_j \left(U_\infty - U_{ji}\right)^2}$$

Equation 2.17

Where U_{ji} is the wake velocity of turbine j investing turbine i.

2.4 Flow Redirection and Induction in Steady State (FLORIS)

FLORIS is an open-source wind farm optimization and control tool, developed by NREL in collaboration with TU Delft, with support from the United States Department of Energy Wind Energy Technologies Office [44] [45]. It is a relatively light tool, which can run in fractions of seconds to find optimal control strategies and estimate the annual energy production of a wind farm. Therefore, it can be used for wind farm design as well as to manage an existing wind farm. FLORIS integrates different wake velocity deficit models, namely the Jensen model, the multi-zone model, the Gaussian model – which is used in the present work –, and the Curl model [46]. FLORIS is capable to consider different wind speeds and directions and turbulence intensities within the same farm, thus reducing the error in forecasting the power output by 18 % [47].

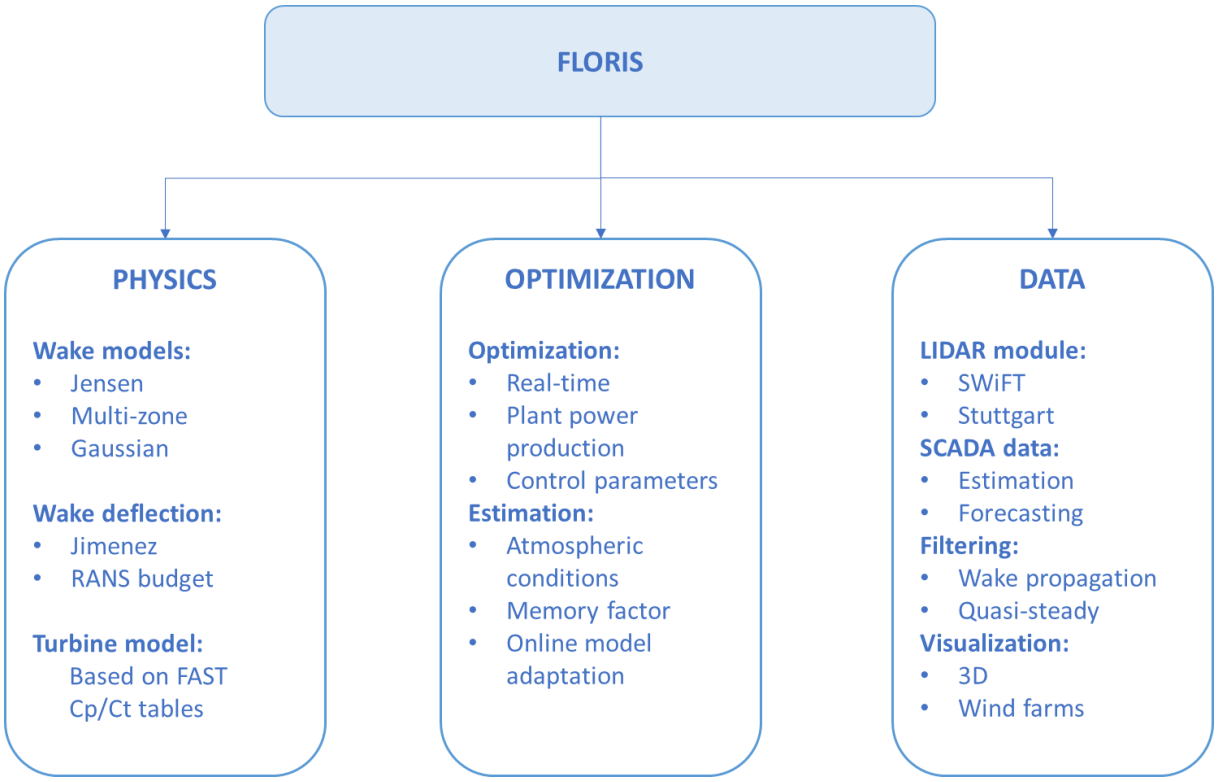

Figure 2.5 - The FLORIS tool set is comprised of three main sections: (1) physics, (2) optimization, and (3) data. Adapted from *[44]*

In FLORIS, a wind turbine is represented as an actuator disk [46], therefore C_p and C_T are defined as a function of the induction factor, a, according to the actuator disk theory [44]:

$$C_p = 4a(1-a)^2$$

Equation 2.18

$$C_T = 4a(1-a)$$

Equation 2.19

Moreover, FLORIS takes as input the wind speed at hub height. Given the wind speed measured at a certain height, h, the wind speed at hub height can be calculated with Equation 2.20 [48].

$$U_{hub} = U_h \frac{\ln {}^{h}/_{z_0}}{\ln {}^{h_{hub}}/_{z_0}}$$

Equation 2.20

Where U_h is the wind speed at the height at which it is measured, h_{hub} and U_{hub} are respectively hub height and the wind speed at hub height, and z_0 is the surface roughness, which depends on the location of the wind turbine.

This tool has been validated though several projects, to compare its results to field data obtained through SCADA [47]. In particular, the comparison between energy ratios is displayed in Figure 2.6, for the case of four turbines in a commercial wind farm.

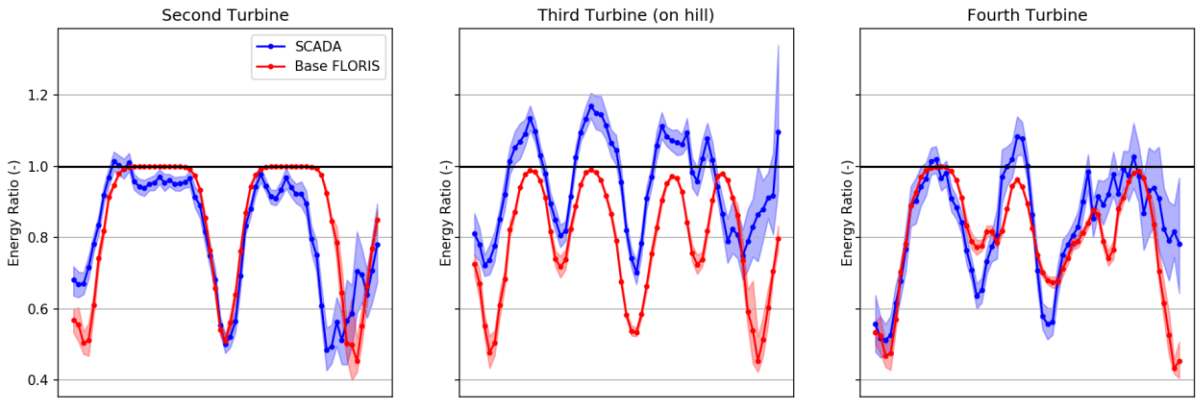

Figure 2.6 - Comparing energy ratio results from FLORIS with field data. Retrieved from *[47]*

Figure 2.7 depicts the velocity profiles calculated with FLORIS using Jensen's model and the Gaussian model. The models are applied to a simple case of a wind farm composed by two 15 MW turbines, with eight diameters between each other. Moreover, the wind is assumed to be coming from west at a wind speed of 10 m/s at hub height. It is noticeable that, as stated above, the Gaussian model ensures a higher level of accuracy than Jensen's model, which is characterized by a discontinuous profile.

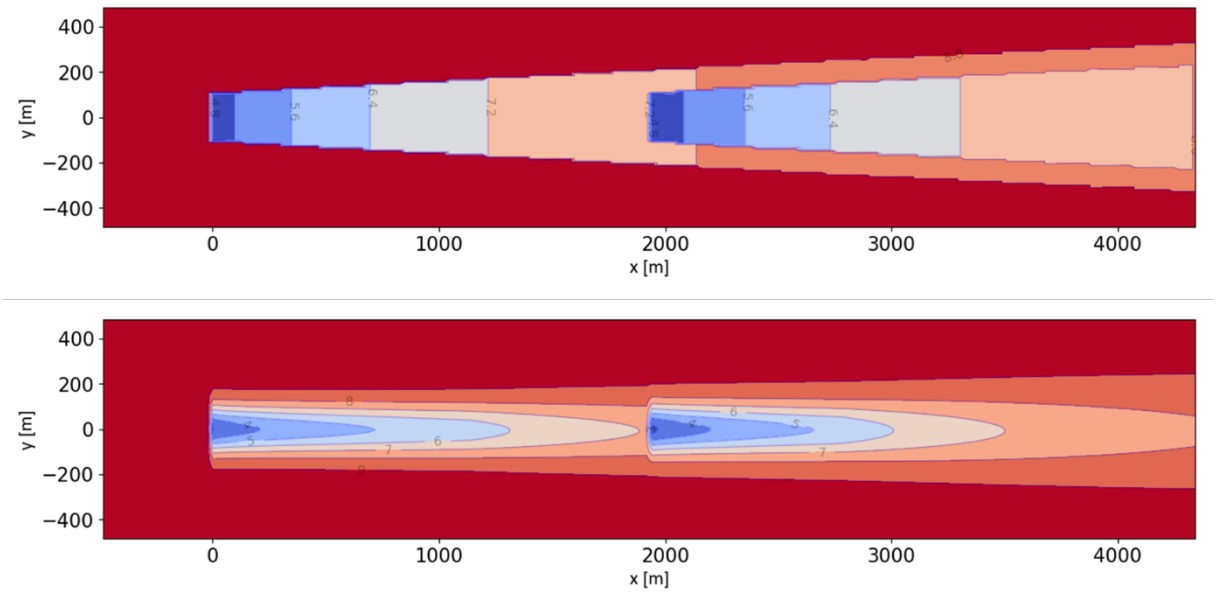

Figure 2.7 - Representation of the velocity deficit calculated on FLORIS with Jensen [above] and Gaussian [below] models

2.5 Offshore Wind Farms Operations and Maintenance

As mentioned above, O&M are responsible for a relevant portion of the LCOE, since the farms are not always accessible due to harsh weather conditions and, when they are, the interventions require special equipment [49]. Therefore, it is of paramount importance to optimize O&M, in order to reduce the LCOE as much as possible.

To be able to discuss O&M for offshore wind farms, some key concepts must be defined:

- *Reliability*: probability that the system will comply with its tasks under given conditions without incurring in failure [49]. Reliability analysis is used for non-repairable and repairable components [50].
- *Availability*: percentage of time during which the system will operate adequately. Availability analysis is used for repairable components [50], as it is highly dependent on maintenance activities. If maintenance is performed regularly and quickly, the availability of a wind turbine can reach values up to 98 % [49].
- *Failure rate*: frequency of occurrence of a component – or more – not being able to perform as required, hence the turbine not being able to produce electricity [51]. Failure rates depend on several factors, such as the location of the wind farm, the type of foundations and drivetrain, maturity of the techniques used [4].
- *Accessibility*: percentage of time during which the site can be accessed by a vessel. It can vary due to weather conditions, namely wind speed and significant wave height [52].

As the offshore wind sector is moving towards deeper waters and bigger turbines, the currently used equipment is facing difficulties to satisfy the demand, namely in terms of crane height, water depth, wave height, sea bottom conditions. Moreover, new solutions will have to consider the environmental impact and the life cycle assessment, as these are aspects are emerging and will be crucial in the future [53].

It is crucial to be able to visit the wind farm often, to prevent failure but, on the other hand, visiting a wind farm too often can be very inefficient and entail extra costs, as vessels can be very expensive [4]. Thus, maintenance scheduling comprises of a trade-off between scheduling frequent interventions to reduce the failure rate and avoiding unnecessary vessels costs. To do so, different types of strategies can be combined:

- *Corrective maintenance*: failure-based strategy, meaning that maintenance is performed only when the failure has already occurred. On the one hand, it is a way to avoid unnecessary maintenance and costs, however unexpected failures may entail even higher costs due to downtime [4].
- *Proactive maintenance*: scheduled maintenance is performed to prevent failures. Predictive and condition-based maintenance are carried out when sensors indicate that a failure is imminent but they are not considered cost-effective [54] [55]. Preventive maintenance is planned and it has several advantages, such as reducing the probability of failures and extending the life of the components. It is performed without knowing when the next failure is going to happen [5].
- *Opportunistic maintenance*: different interventions are carried out at the same time, even if not all of them are strictly necessary in that moment. This can save up to 43 % of preventive maintenance costs [4].

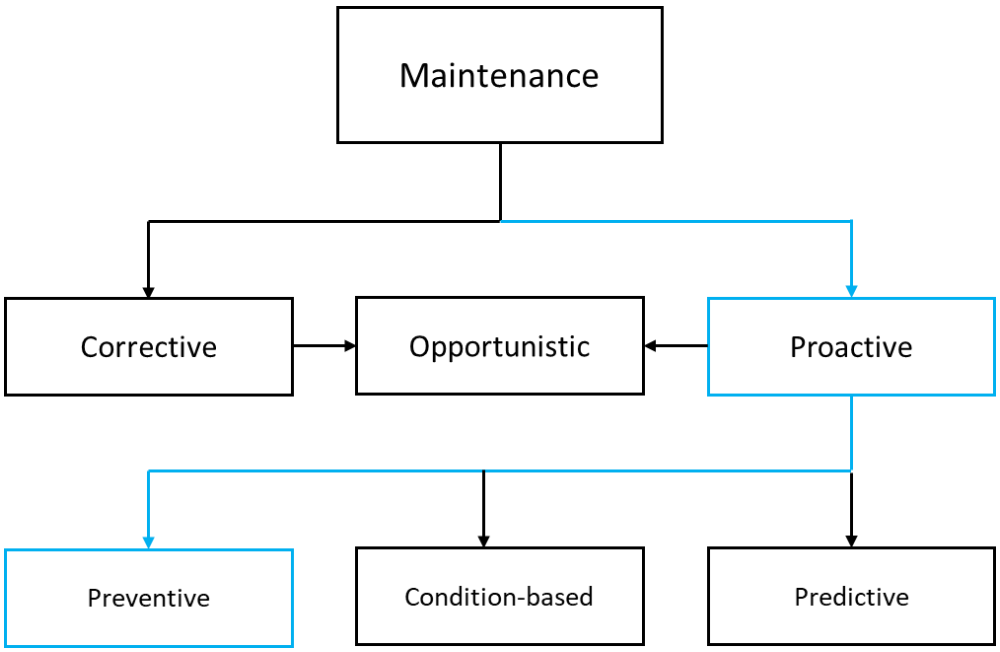

Figure 2.8 - Maintenance strategies. Adapted from *[4]*

Preventive Maintenance

Preventive maintenance is performed to avoid failure of wind turbine components or, at least, reduce the possibility of occurrence [56]. It is a time-based type of maintenance, meaning that it is scheduled in advance, mainly according to weather conditions and personnel availability, thus decreasing downtime and maintenance costs with respect to corrective maintenance [57]. This can be achieved thanks to the fact that time-based maintenance reduces the impact of unfavorable weather conditions and, therefore, avoids longer downtime periods [58].

Preventive maintenance can be based on two criteria: reliability criterium and economic criterium. The reliability criterium is based on fulfilling the objective of meeting the customer's demand; whereas the economic criterium aims to minimize the costs related to maintenance. Both these aspects are critical; therefore, an optimal maintenance strategy should combine them [56].

Weather-Restricted Operations

Preventive maintenance is strongly impacted by weather forecasts, especially because the objects transported are large and expensive, hence the loss would be significant in case they were damaged. Weather-restricted operations planning must comply with standards set by entities such as GL Noble Denton [59] and DNV-OS-H101, Marine Operations, General, DNV (2011), by means of the so-called alpha factor method to estimate uncertainty in the forecasts [60].

The significant wave height is a crucial parameter to consider, when planning activities at sea, like maintenance activities. It is calculated as the average height of the largest 33 % of waves [61]. Weather forecasts are based on data that are received and interpreted; therefore, different meteorologists may provide different forecasts referred to the same moment. As opposed to this, hindcast data allow us to estimate historic significant wave height based on numerical models calibrated with experimental measurements (from wave buoys, satellites, etc.). Figure 2.9 shows a comparison between the two, for every day of year 2011 and Figure 2.10 compares the hindcasted significant wave height with the forecasted one, considering different lead time periods. Both figures highlight a correlation between the hindcasted and the forecasted value, with a lead time up to 72 hours, whereas for longer lead times the correlation is not as significant. In fact, the forecast uncertainty is a function of the lead time [60].

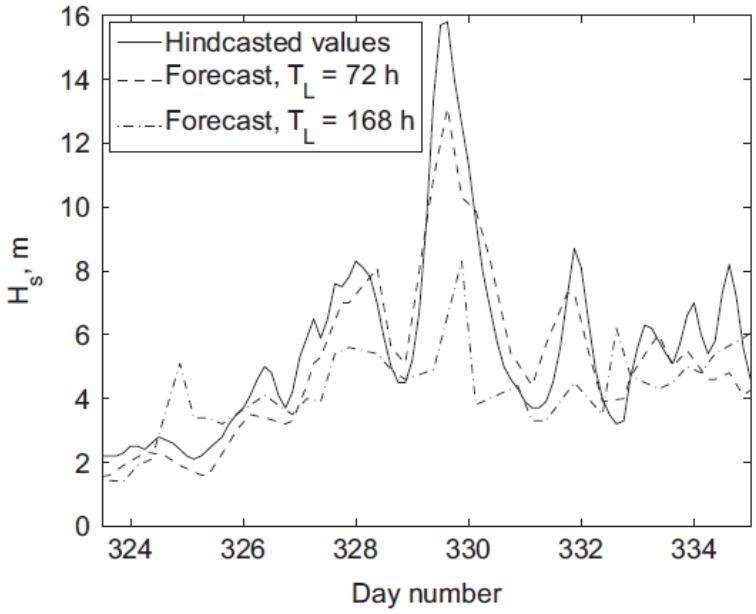

Figure 2.9 - Comparison of forecast and hindcast data. Retrieved from *[60]*

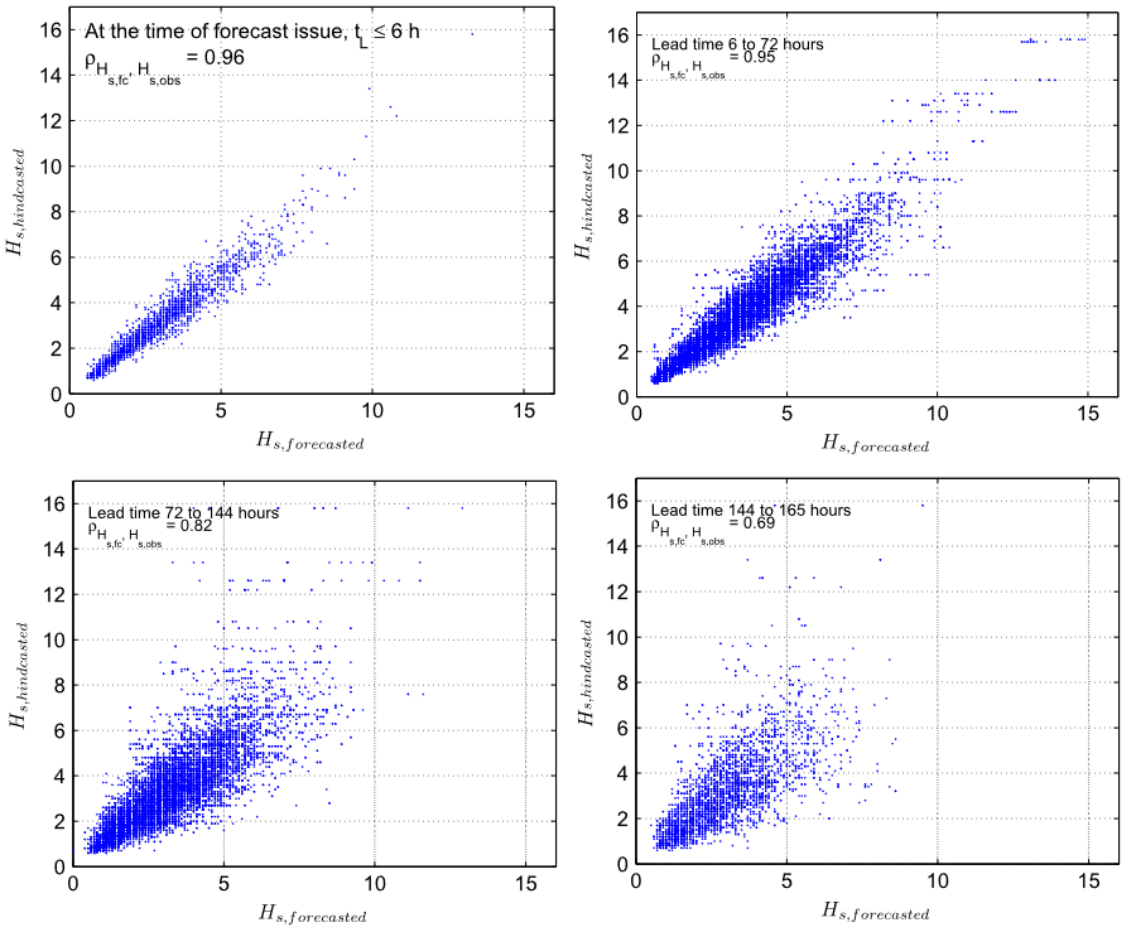

Figure 2.10 - Forecasted versus hindcasted significant wave height. Retrieved from *[60]*

For all types of operations, the reference period is defined as the sum of the planned operation period and the estimated maximum contingency time (which varies between 50 % and 100 % of T_{POP}), as shown in Equation 2.21.

$$T_R = T_{POP} + T_C$$

Equation 2.21

If T_R is lower than 72 hours, the operation is defined as weather-restricted. Both the standards set the operational limit for the significant wave height in weather-restricted operations to:

$$H_{s,oper} = \alpha H_{s,design}$$

Equation 2.22

Where α is a parameter ≤ 1, which is dependent on the duration of the operation and the level of forecasting [60]. Guidelines from DNV suggest values for this parameter, depending on the design significant wave height, the planned operation period, and the accuracy of the weather forecast. For Level A forecasts with a meteorologist at site, the values are depicted in Table 2.3. For the present thesis, the hindcast is assumed to be perfectly accurate and the planned operation period is equal to 10 hours, hence this factor can be set to 0.95. Wave height is, indeed, the most important parameter [62], hence it is of paramount importance to be able to forecast it accurately and take it into account.

Table 2.3 - Alpha factor for waves, with monitoring and Level A forecasts with meteorologist. Retrieved from *[63]*

	Design Wave Height [m]			
Planned Operation Period [h]	**H_s = 1**	**H_s = 2**	**H_s = 4**	**H_s ≥ 6**
T_{POP} ≤ 4	0.9	0.95	1.0	1.0
T_{POP} ≤ 12	0.78	0.91	0.95	0.96
T_{POP} ≤ 24	0.72	0.84	0.87	0.90

3. Methodology and Case Study

3.1 Wind Farm Characteristics

The wind farm analyzed in this case study consists of 25 turbines, disposed in a squared layout with a distance equal to eight diameters between one another, as shown in Figure 3.1. As current developments in turbines size are going towards bigger machines, the IEA 15 MW Reference Wind Turbine is chosen and its characteristics are summarized in Table 3.1. Therefore, the total capacity of the wind farm is equal to 375 MW.

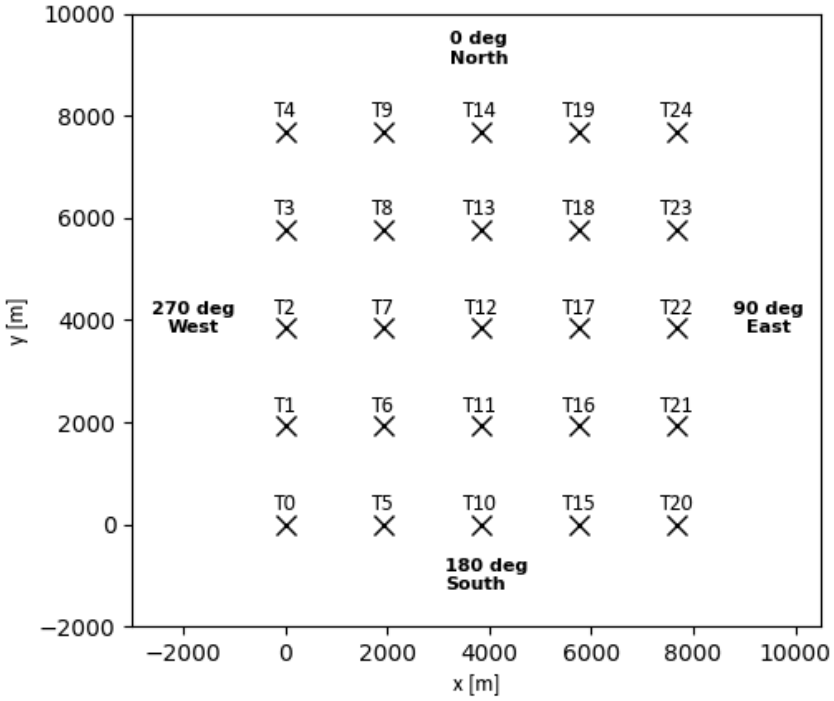

Figure 3.1 - Wind Farm Layout

Table 3.1 - IEA 15 MW Reference Turbine parameters. Adapted from *[64]*

Parameter	Unit	Value
Cut-in wind speed	m/s	3
Rated wind speed	m/s	10.59
Cut-out wind speed	m/s	25
Hub height	m	150
Rotor diameter	m	240

The wind farm is situated 25 km off the shores of Viana do Castelo, Portugal. This is because WavEC has extensive weather data available for the location. Moreover, it is a proven site for the floating offshore wind technology, as the world's first semi-submersible FOWF is located there, as mentioned in State of the Art.

The weather data provided include hourly data for wind speed [m/s] and wind direction [°] at 10 m height, and significant wave height [m], from 1992 to 2012. These hindcast data is used to develop an improved preventive maintenance strategy for the wind farm, considering the influence of wake effect on downtime energy losses. Because the wind farm is located offshore, the surface roughness, z_0, necessary to calculate the wind speed at hub height, since the data available are measured at 10 m height, can be set to 0.0002 m [48].

3.2 Weather Data Analysis

As it will be demonstrated later, wind direction is the most important variable to consider when deciding on which turbines maintenance should be carried out on a specific day. For this reason, the wind direction variation throughout the day is analyzed to find a trend. To do so, the data are separated into months, only including months between April and October as it is the workable period. Moreover, within each month, days are furtherly divided into sixteen groups, depending on the wind speed and direction at 6 a.m.. The thresholds of each group are summarized in Table 3.2.

Table 3.2 - Wind direction and wind speed groups

Wind speed groups (V) [m/s]	0 – 3	3 – 6.5	6.5 – 10	10 – 15
Wind direction groups (D) [°]	315 – 45 (North)	45 – 135 (East)	135 – 225 (South)	225 – 315 (West)

Wind speeds above 15 m/s are not included, since it is not possible to carry out maintenance under such harsh wind conditions. Moreover, for visualization purposes, only workable days are plotted and the plots follow a color code based on the maximum wind direction variation throughout each day.

Figure 3.2 to Figure 3.8 show these plots, for all the months in which maintenance is carried out. These graphs highlight a strong variability of wind direction throughout the day, since several days have a variation between 90 ° and 180 °. Therefore, to decide on which turbines to operate, it is important to select the set to maintain based on a proper representation of the wind directions that occur during the day. To do so, a representative wind direction is calculated, as well as a representative wind speed.

The results obtained highlight that, early in the morning, wind tends to come from East during Spring and Fall, whereas it comes from North on most days approaching Summer (Table 3.3). Moreover, Table 3.4 depicts the occurrence of the three ranges of wind direction excursion. As visible in the figures, most of the days present a significant excursion, between 90 ° and 180 °. Consequently, it is not feasible to plan maintenance based on the

wind conditions at 6 a.m.. On the contrary, it is of paramount importance to consider the strong variation of this parameter during the day, as its influence on the set of wind turbines to maintain is significant.

Nevertheless, when the maximum difference belongs to the 90 °- 180 ° group, there is a trend that is visible: the wind comes from north in the morning, then the direction changes for approximately two hours to east, south, west, and finally goes back to coming from the north. The pattern is repeated more than once throughout the day and it is happening during the whole period analyzed. This observation can be used in future works, to apply a similar algorithm with weather forecasts, instead of hindcasting. Moreover, it is possible to observe that in Summer, when the wind comes from West in the morning, it is more likely to have small direction variations during the day.

Concerning the velocity, wind speeds above rated speed almost never occur in summer, whereas they are occurring in other seasons, although in a low share of days. Moreover, up until August the wind speed is mostly below 6.5 m/s at 6 a.m., whereas in September and October the occurrence of wind speeds up to 10 m/s is more frequent.

Table 3.3 - Wind direction at 6 a.m. per month [%]

	North	East	South	West
April	31%	48%	15%	7%
May	39%	31%	19%	12%
June	52%	23%	15%	11%
July	62%	15%	11%	12%
August	60%	18%	11%	12%
September	39%	39%	14%	8%
October	29%	57%	10%	4%

Table 3.4 - Wind direction variation during the day per month [%]

	0 - 30 °	30 - 90 °	90 - 180 °
April	12%	28%	60%
May	14%	30%	56%
June	15%	29%	56%
July	14%	28%	59%
August	13%	25%	62%
September	10%	19%	71%
October	14%	33%	53%

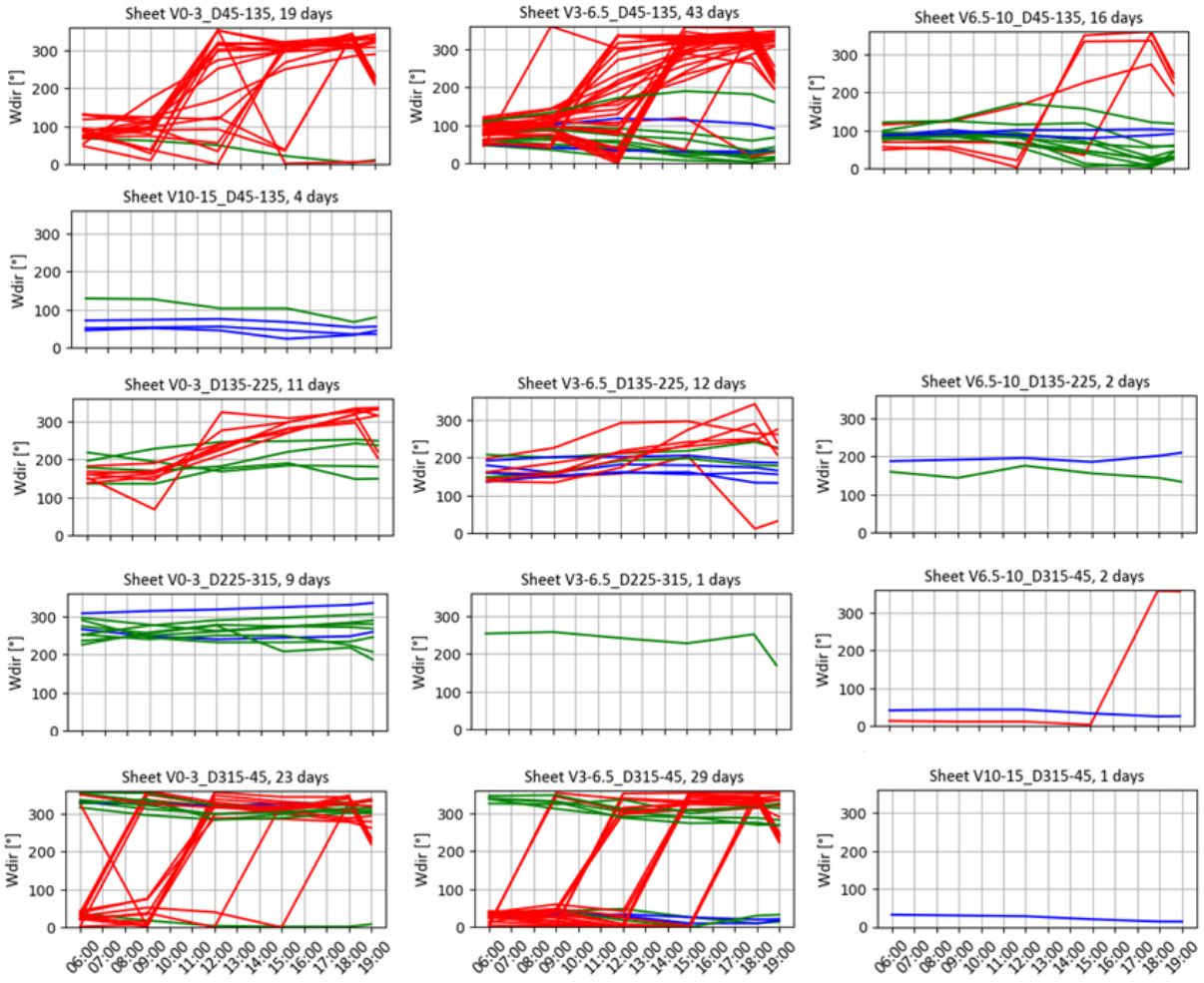

Figure 3.2 - Wind direction trends (April, 172 days). Blue is used for days that have a maximum difference between 0 and 30 degrees; green is used if the difference is between 30 and 90 degrees and red is used if it is between 90 and 180 degrees

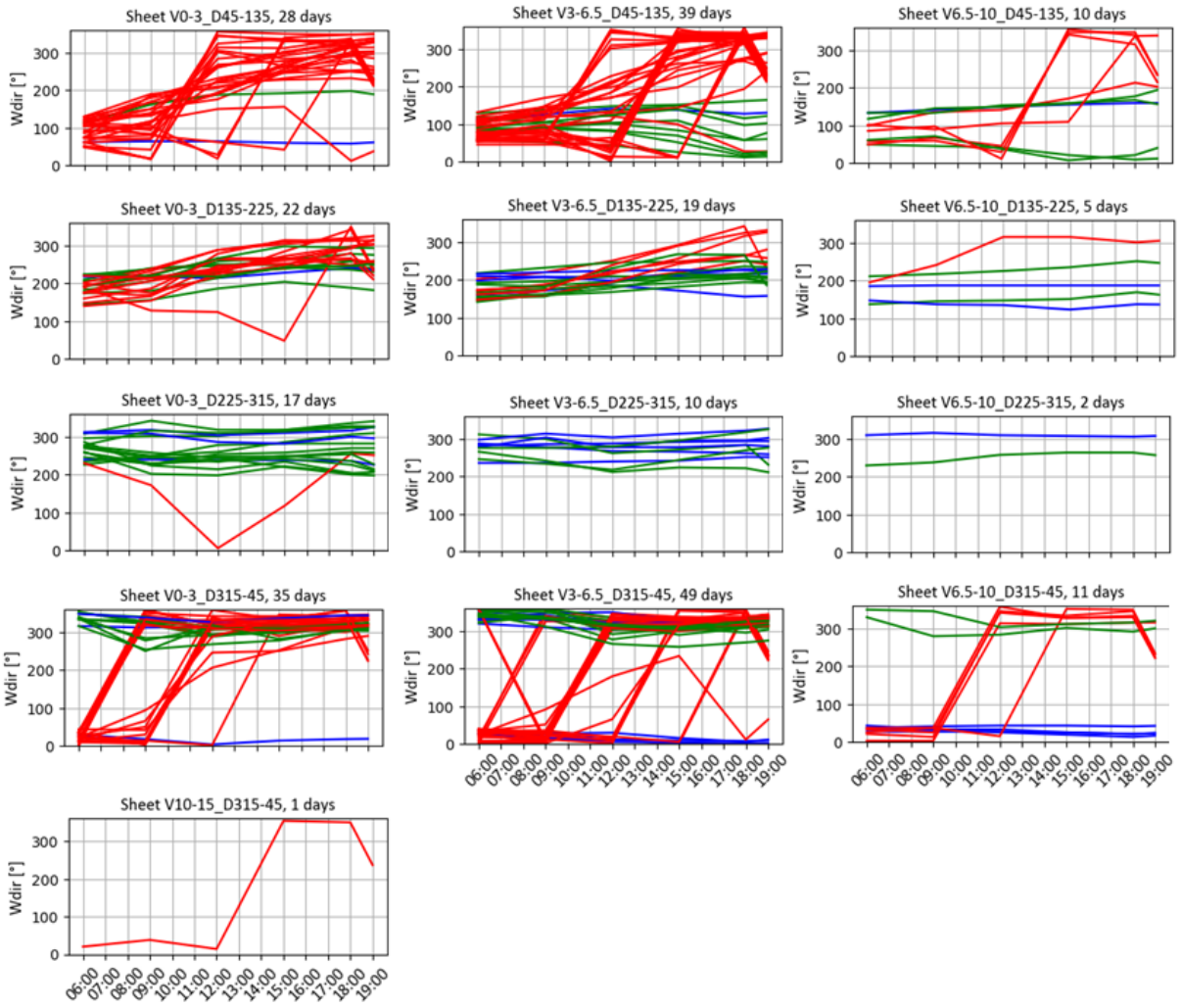

Figure 3.3 - Wind direction trends (May, 248 days). Blue is used for days that have a maximum difference between 0 and 30 degrees; green is used if the difference is between 30 and 90 degrees and red is used if it is between 90 and 180 degrees

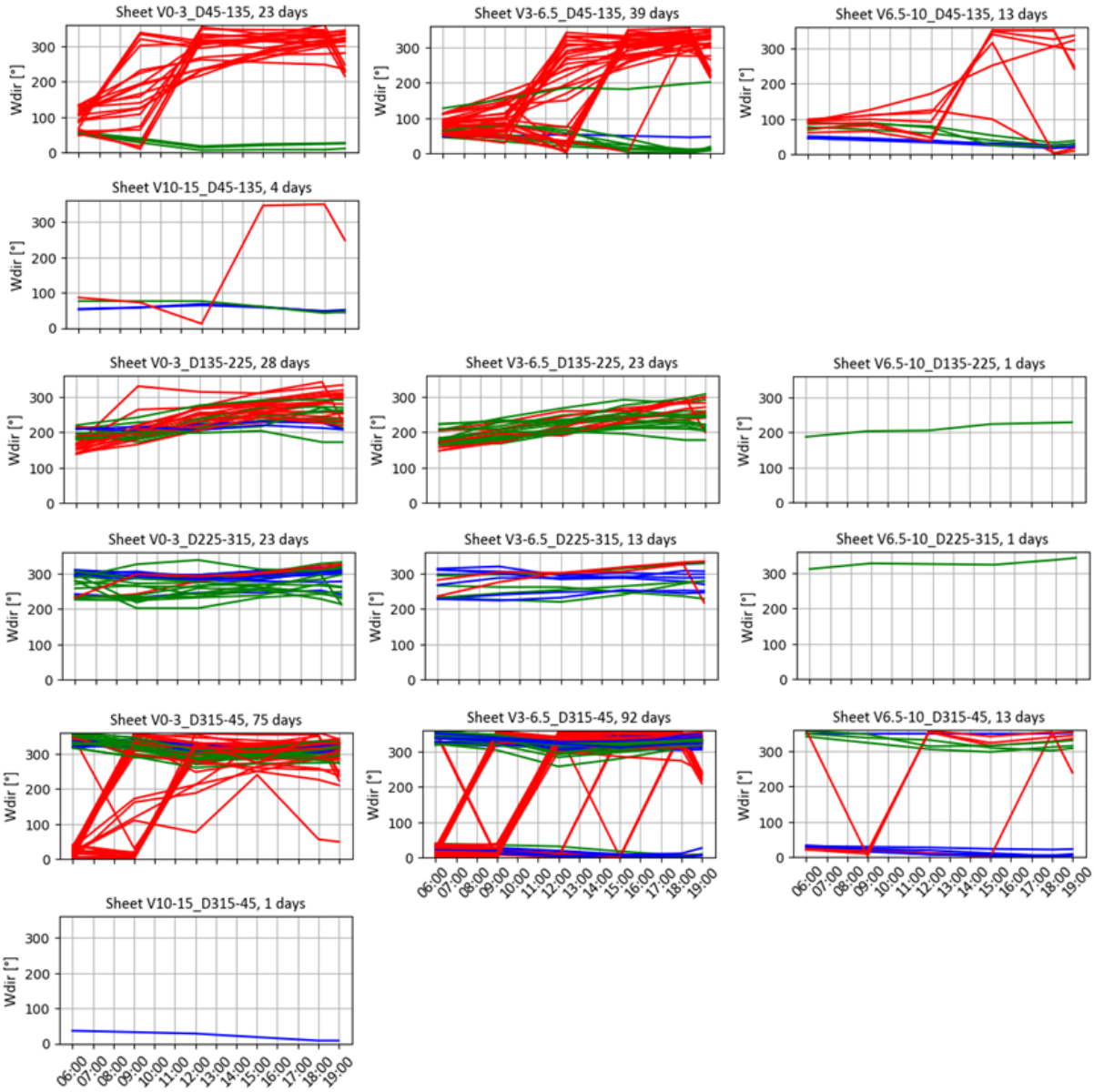

Figure 3.4 - Wind direction trends (June, 349 days). Blue is used for days that have a maximum difference between 0 and 30 degrees; green is used if the difference is between 30 and 90 degrees and red is used if it is between 90 and 180 degrees

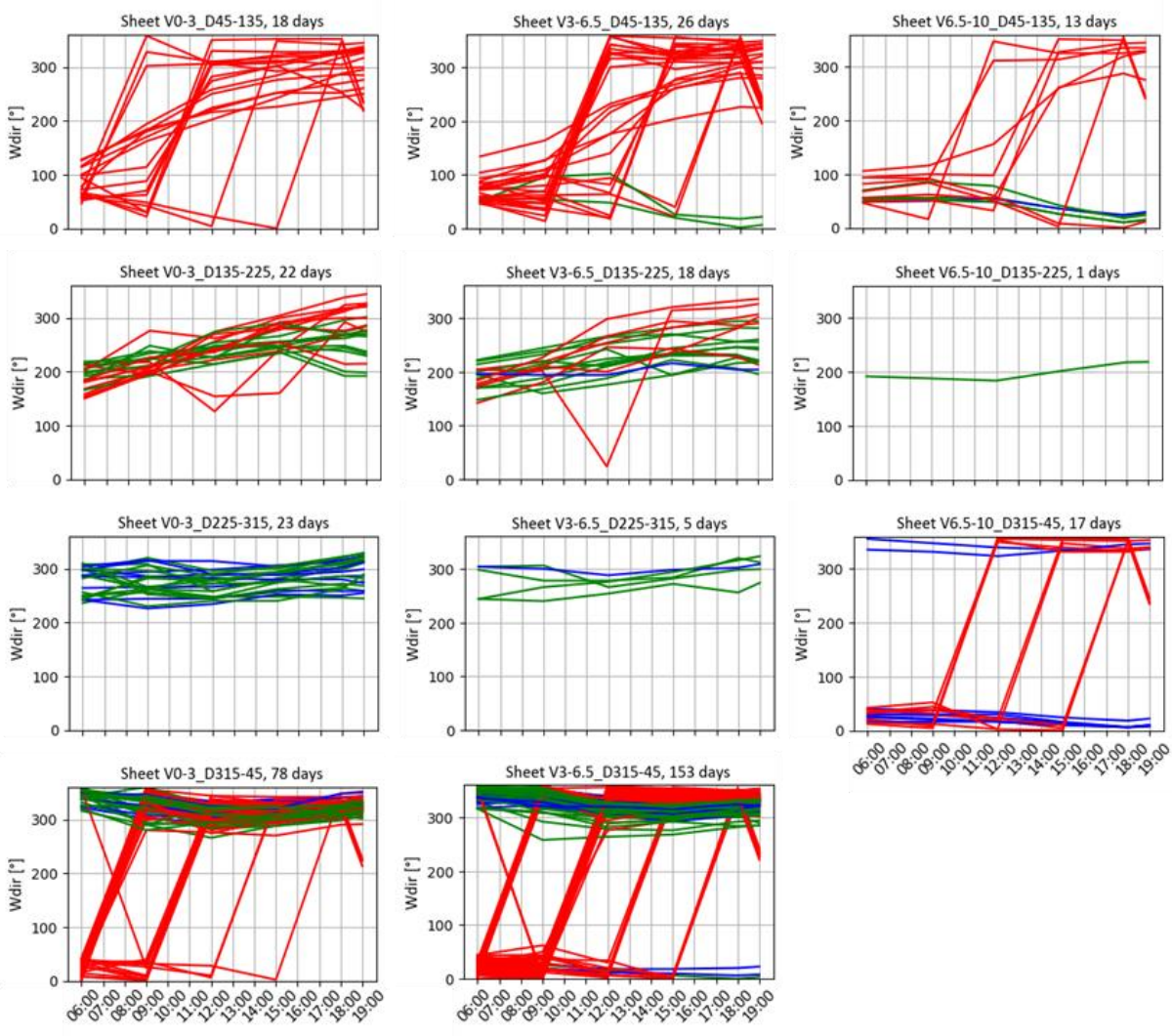

Figure 3.5 - Wind direction trends (July, 374 days). Blue is used for days that have a maximum difference between 0 and 30 degrees; green is used if the difference is between 30 and 90 degrees and red is used if it is between 90 and 180 degrees

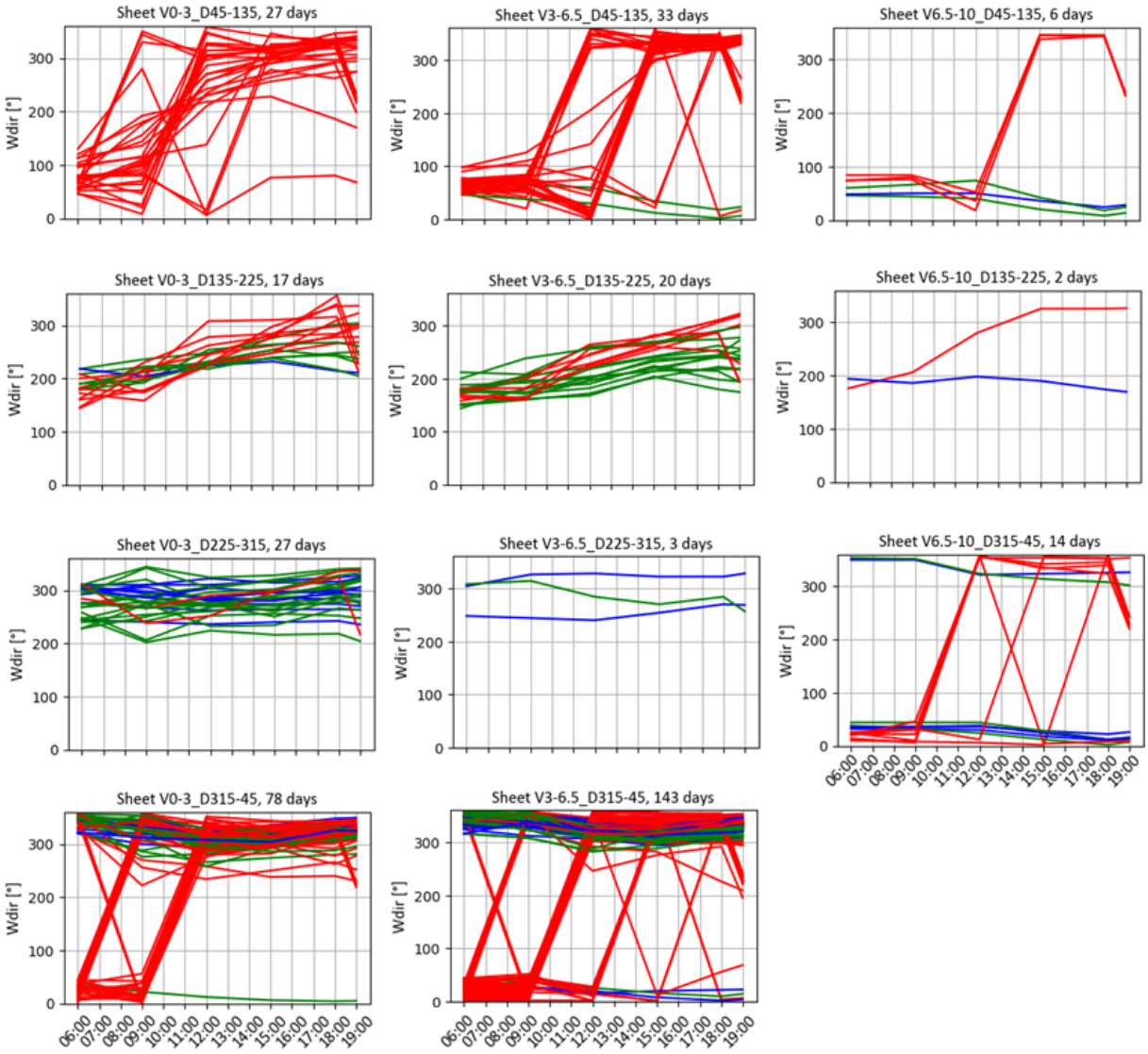

Figure 3.6 - Wind direction trends (August, 370 days). Blue is used for days that have a maximum difference between 0 and 30 degrees; green is used if the difference is between 30 and 90 degrees and red is used if it is between 90 and 180 degrees

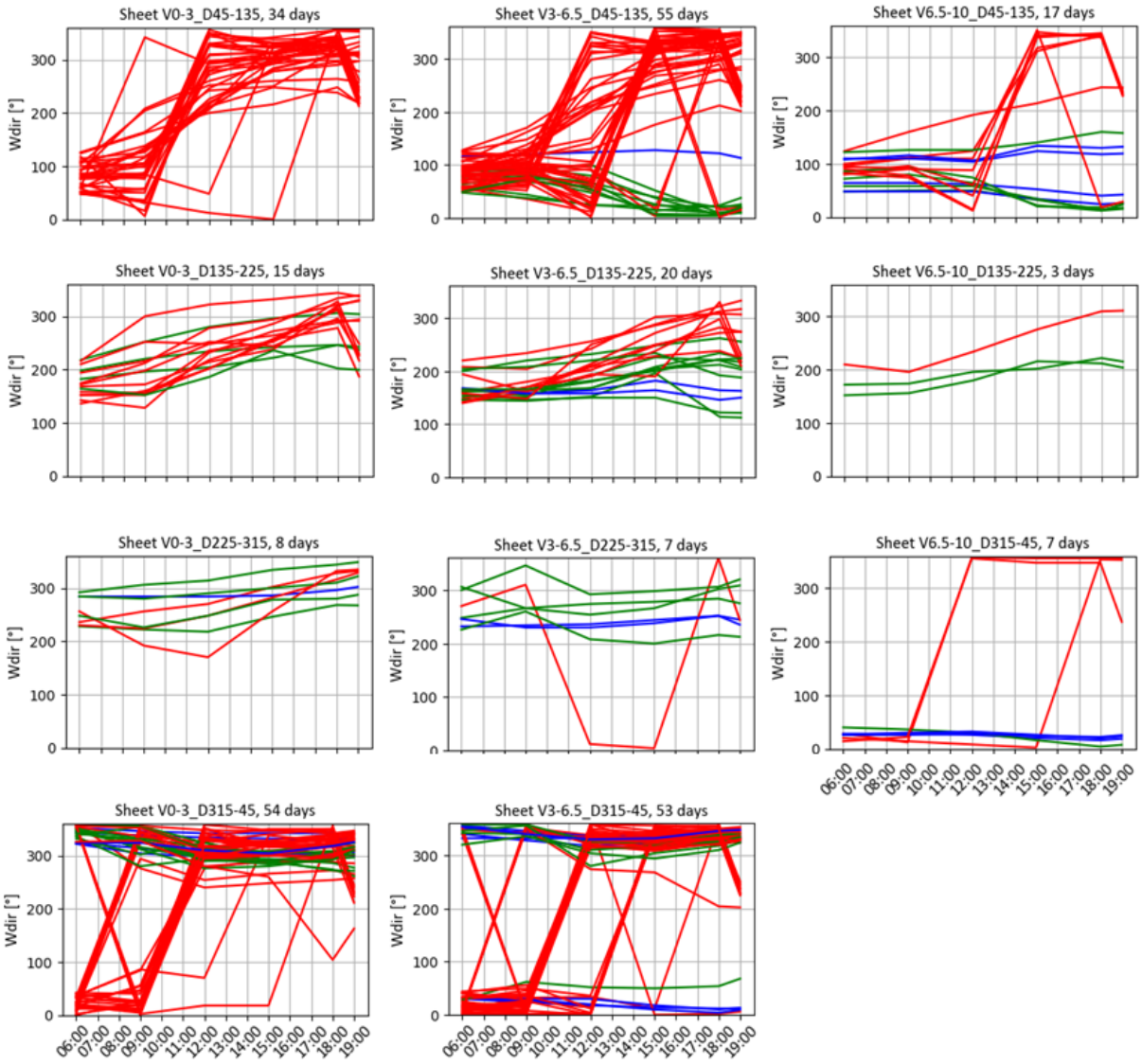

Figure 3.7 - Wind direction trends (September, 273 days). Blue is used for days that have a maximum difference between 0 and 30 degrees; green is used if the difference is between 30 and 90 degrees and red is used if it is between 90 and 180 degrees

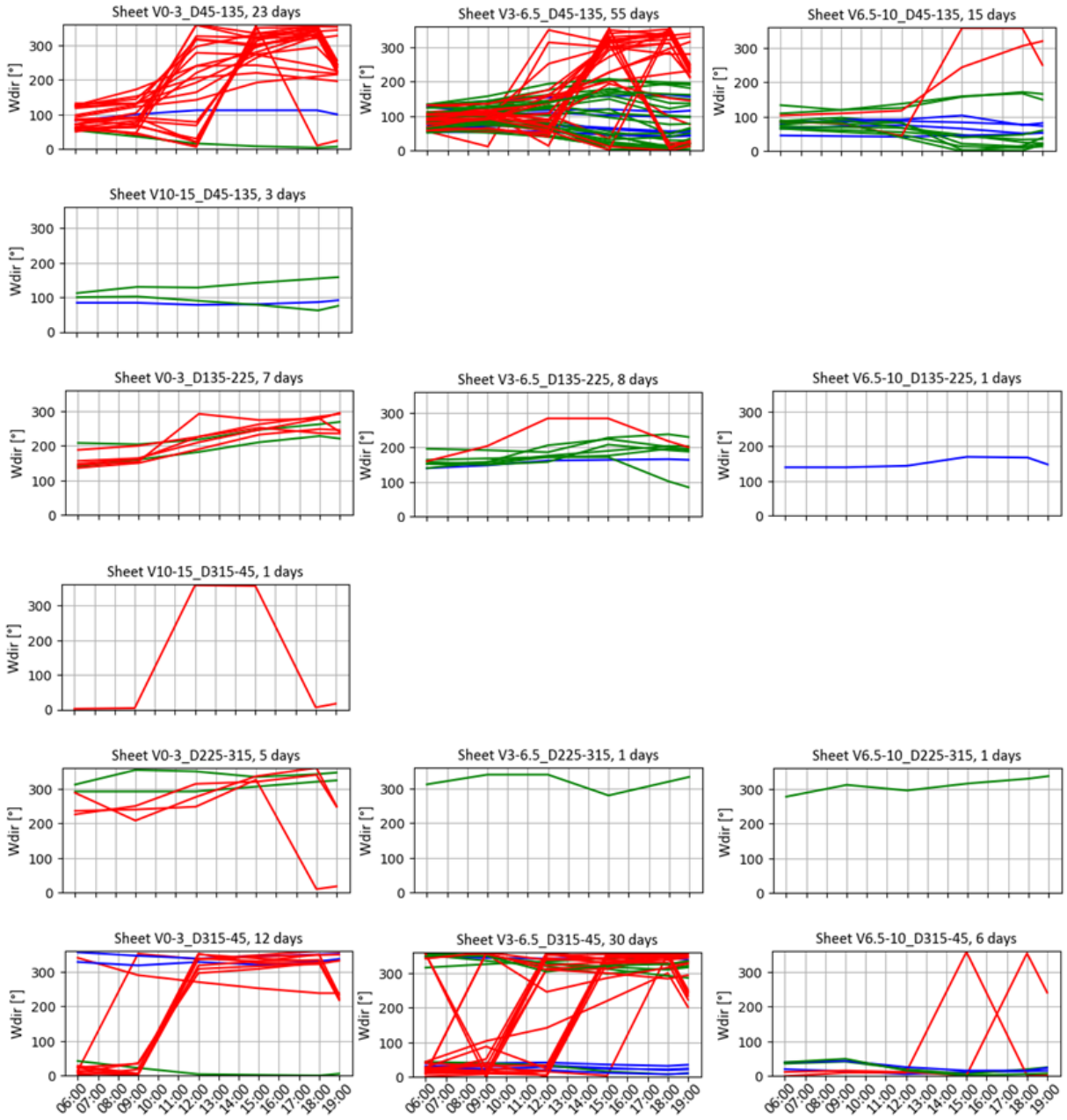

Figure 3.8 - Wind direction trends (October, 168 days). Blue is used for days that have a maximum difference between 0 and 30 degrees; green is used if the difference is between 30 and 90 degrees and red is used if it is between 90 and 180 degrees

To calculate the representative wind direction, the directions are separated into the sectors mentioned above. Moreover, only values that belong to the domain H are taken (from 6 am to 19 pm), as Equation *3.1* shows.

$$H = \{6; 7; 8; 9; 10; 11; 12; 13; 14; 15; 16; 17; 18; 19\}$$

Equation 3.1

Within the domain defined, Equation 3.2 shows that the mode, $\mu_{0,}$ is taken. In this case the mode is the modal class, as in the one of the four groups described that has the highest frequency, therefore it is a set of values. Finally, the median of the modal class is chosen as representative wind direction as displayed in Equation 3.3.

$$\{Wdir_{representative\ group}\} = \mu_0 \left\{W_{dir,groups}\big|_H\right\}$$

Equation 3.2

$$Wdir_{representative} = Mdn\{Wdir_{representative\ group}\}$$

Equation 3.3

The representative wind speed is calculated as shown in Equation 3.4. Since the power produced when the wind speed is lower than the rated wind speed, is proportional to the cube of the wind speed itself, the representative value chosen is the value of velocity that averages the cube of wind speed.

$$Uw_{representative} = \sqrt[3]{(U_w^3)_{avg}} = \sqrt[3]{\frac{\sum_{hour=6}^{19} U_{w,hour}^3}{Length(H)}} = \sqrt[3]{\frac{\sum_{hour=6}^{19} U_{w,hour}^3}{14}}$$

Equation 3.4

This is a significant difference compared to the work that the present thesis builds up on, which used the mean values of wind speed and direction and representative, concluding that this method to calculate wind direction is not correct, as it does not allow to properly select the best set of turbines to maintain every day [65].

Figure 3.9 shows the importance of having a good approximation for representative wind speed and direction: due to the strong variability of the wind condition within a day, it is crucial to obtain values that properly represent the day, to choose on which set of turbines to operate. In fact, Figure 3.10 represents, along with hourly and representative wind direction, the mean and median value of the same parameter. It is noticeable that the difference is significative, thus using another method to calculate the representative wind direction would cause significant differences in terms of turbines maintained and downtime losses. The representative wind direction is a key parameter, since the set of turbines to be maintained on each day depends on it.

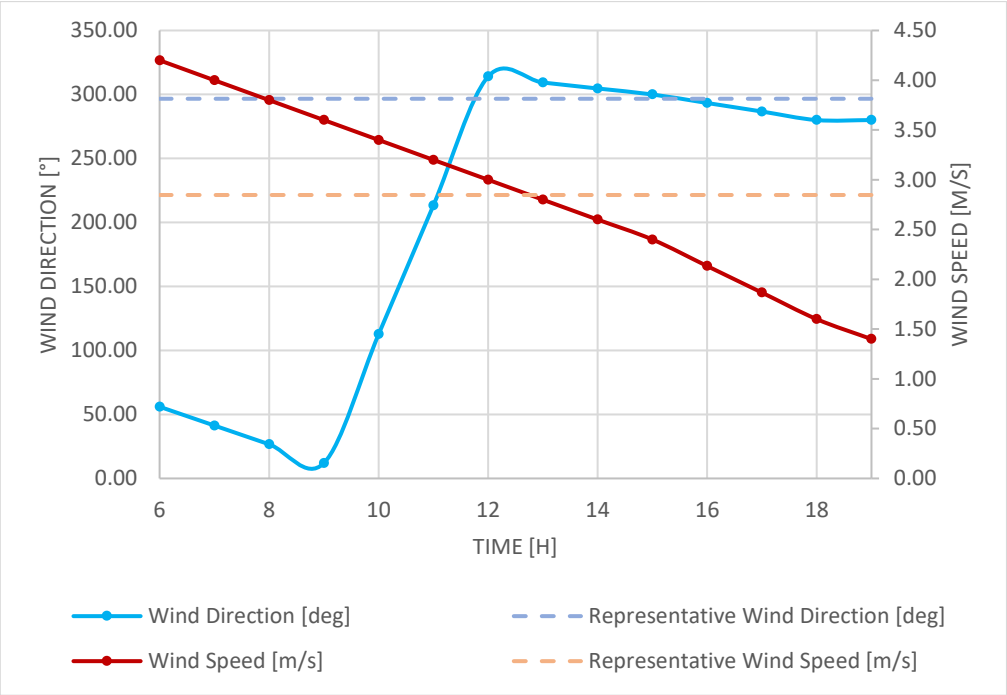

Figure 3.9 - Representative and hourly wind conditions for 19th October 1992

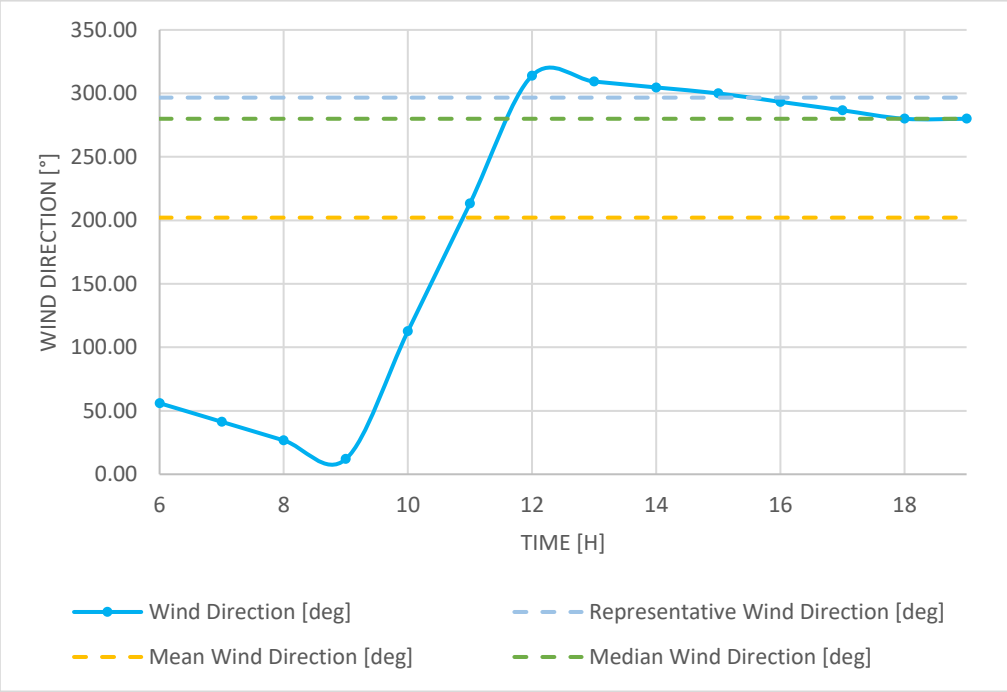

Figure 3.10 - Wind direction for 19th October 1992

3.3 Conditions for Maintenance

Information provided by WavEC suggests that each turbine requires 80 hours of preventive maintenance per year and that maintenance should be performed in shifts of 10 hours during daylight (between 8 a.m. and 8 p.m.). Moreover, the Crew Transfer Vessel (CTVs) that are used have some limitations in terms of maximum wind speed and significant wave height at which they can operate:

- The wind speed at 10 meters height must be below 15 m/s;
- The significant wave height must be lower than 1.5 m (for Regular CTVs).

A day is considered workable if the wind speed and the significant wave height are below the limits defined during the whole workable window, from 8 a.m. to 8 p.m.. This is because, although a shift lasts 10 hours, safe weather conditions need to be ensured while the CTV goes from the port to the wind farm and back, as well as while it is moving from a turbine to another to transport technicians. Moreover, maintenance is assumed to be performed only between April and October, as weather conditions tend to be unfavorable during the rest of the year. An assumption is made that technicians and CTVs are always available to work, when the decision on whether to operate or not is made in the morning. Furthermore, for simplicity it is assumed that downtime starts and finishes at the same time for every turbine, although in reality there is a time displacement due to the fact that the technicians need to be transported from one turbine to another.

Figure 3.12 displays the workable days that are available for maintenance with Regular CTVs. As CTVs typically have a capacity between 12 and 16 technicians [66] and internal information from WavEC suggests 2 to 3 technicians are required to perform preventive maintenance on a single turbine, with a single CTV it is possible to maintain 5 turbines at a time. Moreover, this number of turbines guarantees a high probability that all the turbines receive the hours of maintenance they require throughout the year [65]. This means that, for all the 25 turbines to receive 80 hours of maintenance, at least 40 workable days per year are required, if it is assumed to perform maintenance whenever it is possible. This approach is not optimal, as the wind speed limit for a day to be workable is well above the rated wind speed. Therefore, carrying out maintenance whenever possible can lead to a significant downtime energy loss, on days with such wind speeds. Moreover, despite the high probability of having enough workable days, not all years have 40 workable days. According to internal data about energy prices and CTV cost, using a second CTV to operate on more turbines at the same time would not be cost convenient, as the second CTV's cost would not be compensated by the increase in AEP.

Therefore, to implement a non-binary criterium that allows to reduce the energy losses due to downtime, novel CTVs are contemplated. In particular, three CTVs that can operate with significant wave heights over 2 meters are already available in the market: FSC2710 by Damen [67] [68], WB-18 Wind by Wallaby Boats [69] and a CTV designed by Louis Dreyfus Armateurs for the Saint-Nazaire Wind Farm [70]. These CTVs are presented in Figure

3.11. As noticeable in Figure 3.12, the workable days increase significantly thanks to these CTVs, and non-binary criteria can be implemented to furtherly reduce downtime energy losses.

Figure 3.11 - Novel CTVs. From left to right: FSC2710 by Damen, WB-18 Wind by Wallaby Boats and CTV designed by Louis Dreyfus Armateurs for the Saint-Nazaire Wind Farm

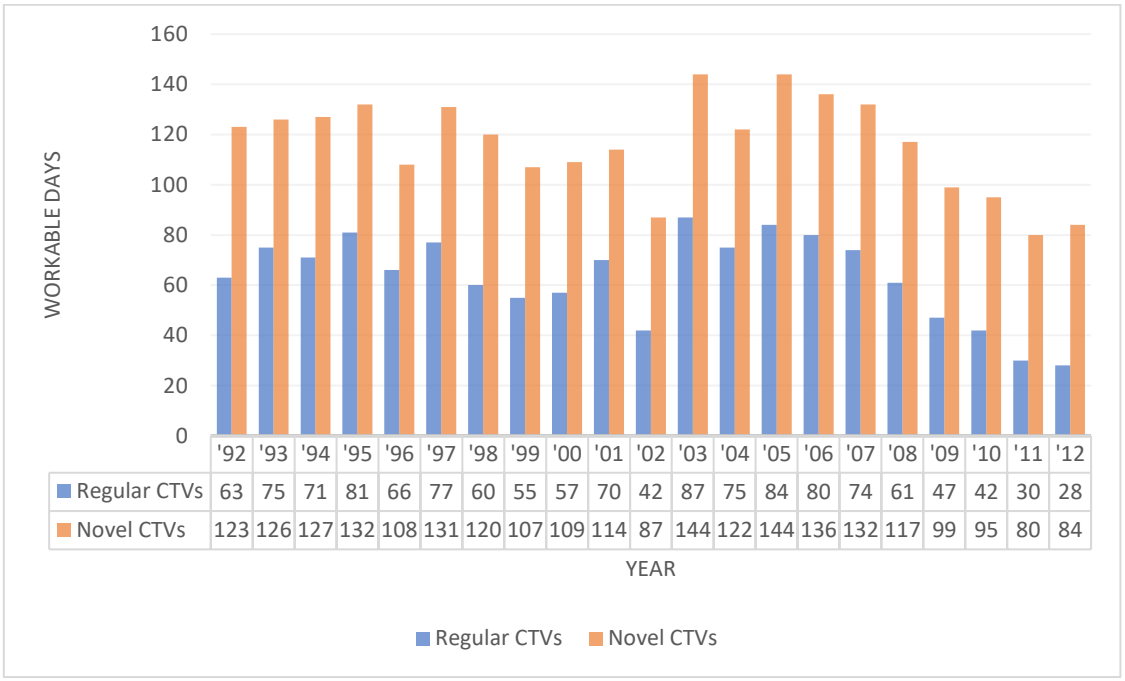

	'92	'93	'94	'95	'96	'97	'98	'99	'00	'01	'02	'03	'04	'05	'06	'07	'08	'09	'10	'11	'12
Regular CTVs	63	75	71	81	66	77	60	55	57	70	42	87	75	84	80	74	61	47	42	30	28
Novel CTVs	123	126	127	132	108	131	120	107	109	114	87	144	122	144	136	132	117	99	95	80	84

Figure 3.12 - Workable days with Regular and Novel CTVs

3.4 Wind Farm Aerodynamics and Servicing

In the present work, FLORIS is mainly used for two scopes: ranking all the possible sets of turbines based on their associated energy losses due to downtime, and calculating the AEP and yearly energy losses caused by maintenance when preventive maintenance is scheduled with different logics and algorithms. The following

steps are completed under the assumption that, if a turbine is switched off, it behaves as if it did not exist, hence it is removed from the layout.

Ranking of Best Sets of Turbines

Firstly, the size and layout of the wind farm, the number of turbines to be maintained at the same time, and a wind speed and direction are given as an input to the function, which creates a list that contains all the possible sets of turbines. Then, FLORIS is used to calculate the power produced when all twenty-five turbines are on and when each of the sets is switched off, hence the power loss associated with turning off each set of turbines. Therefore, the sets are ranked from the one with the lowest losses to the one with the highest in a static table. Figure 3.13, valid for the specific machine that was available and was used to conduct the simulations, shows that the computational time significantly increases when increasing the size of the sets of turbines, and the curve can be approximated with the equation displayed on the graph. Hence, this function was tested to prove its functioning with a small group of simultaneously maintained turbines, to reduce the computational time in the testing phase.

These tests highlighted that the ranking depends mainly on the wind direction, and it is not remarkably influenced by wind speed, confirming what had been observed in the work that the present thesis builds up on [65]. Therefore, when scaling up to five or six turbines simultaneously maintained, the ranking was computed for just two wind speeds, to verify that its influence is negligible, and different wind directions. In particular, the wind speeds considered are 8 m/s (below rated wind speed) and 8.5 m/s at a height of 10 meters, which means that at hub height the speed is equal to the rated value. Concerning the wind directions, the ranking is calculated from 0 to 360 degrees, with a step of 5 degrees.

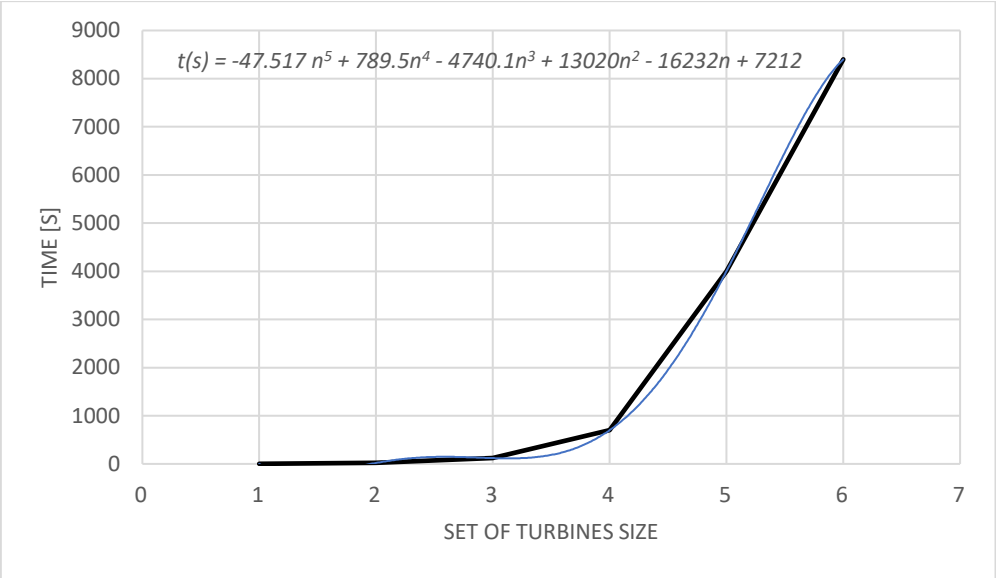

Figure 3.13 - Computational time to rank the sets of turbines as a function of the number of turbines simultaneously maintained (n)

Since the wind turbines are placed in a squared layout, symmetries apply, and it is not necessary to do this ranking for all the directions. In fact, a square has four lines of symmetry, thus it is only necessary to run the function between 9 and 45 degrees, and then apply the symmetries. To facilitate the process, it was decided to run the function between 0 and 85 degrees, such that only rotational symmetry needs to be implemented. The symmetrical nature of the layout is visible in Figure 3.14. Said figure shows the wind farm layout highlighting that, at the same wind speed, the power loss that is caused by turning off the turbine 'T7' when the wind comes from north is the same that is caused by turning off the turbine 'T11'. Figure 3.15 shows that there is also a symmetry with respect to the diagonals of the square. The symmetry is implemented with a Python script as well, to make the process lighter and automatized. An example of the rankings obtained is displayed in Table 3.5, and the associated percentual losses are shown in Table 3.6 shows that, depending on the wind direction, the difference in percentage of power loss can vary significantly. This can also be seen in Figure 3.15, which represents the power produced at each wind direction by 25 turbines, and then by switching off the best set and the worst set. For certain angles, the difference in power production is higher than for others and, in general, the angle has a strong influence on the power that is produced. Therefore, it is crucial to calculate a representative wind direction that properly represents the day, as an imprecise calculation can lead to a wrong selection of the set of turbines to maintain, and thus a significant variation of energy loss due to downtime.

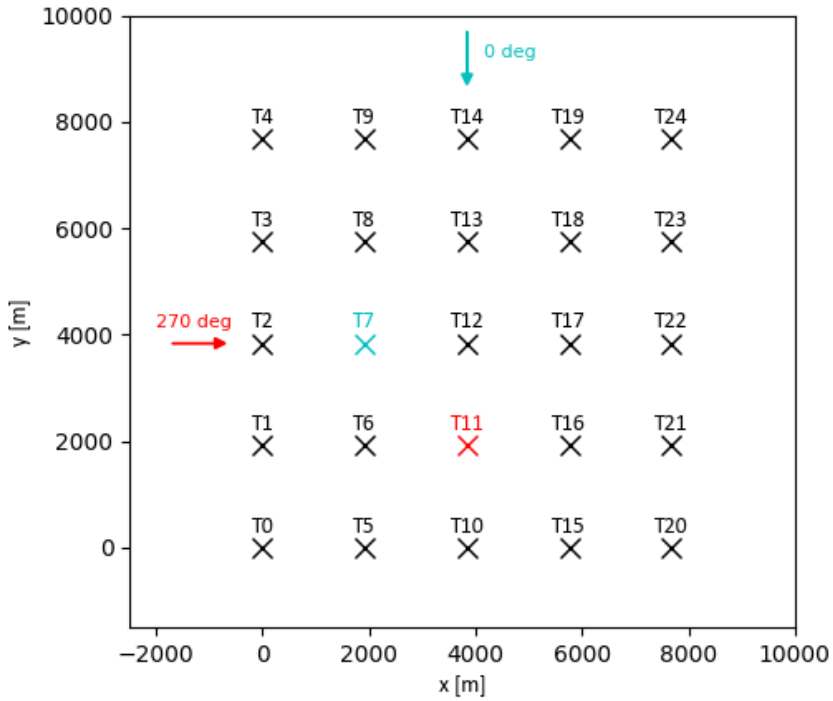

Figure 3.14 - Wind farm layout highlighting symmetry

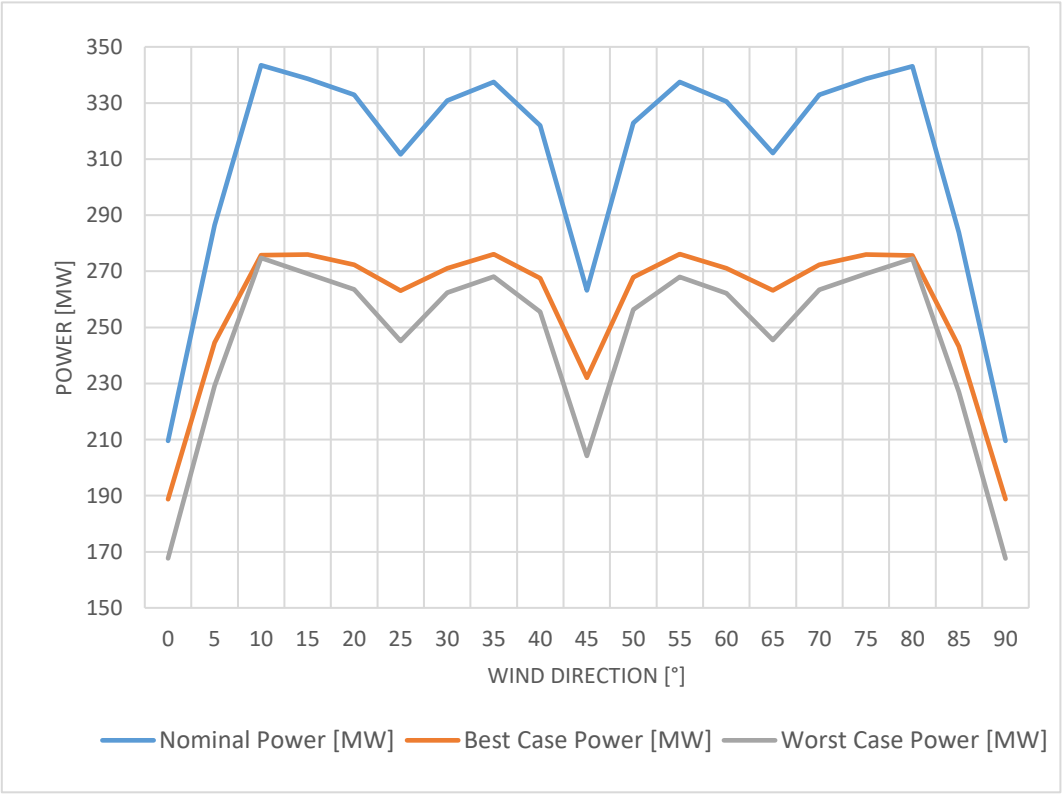

Figure 3.15 - Comparison of Power Production with different wind directions

Table 3.5 - Ranking of sets of turbines with n = 5

Ranking	0 degrees	15 degrees	30 degrees	45 degrees
1	(1, 6, 11, 16, 21)	(0, 10, 13, 14, 24)	(7, 11, 12, 17, 23)	(6, 7, 8, 11, 16)
2	(1, 6, 16, 18, 21)	(0, 5, 10, 14, 24)	(6, 7, 12, 17, 23)	(6, 8, 11, 16, 18)
3	(1, 11, 16, 18, 21)	(0, 14, 18, 19, 24)	(1, 7, 12, 17, 23)	(6, 7, 8, 16, 18)
4	(6, 11, 16, 18, 21)	(0, 14, 15, 18, 19)	(7, 12, 15, 17, 23)	(6, 8, 11, 13, 16)
5	(1, 6, 16, 21, 23)	(0, 5, 18, 19, 24)	(7, 12, 17, 22, 23)	(6, 7, 8, 16, 17)
…				
53126	(0, 1, 2, 3, 4)	(2, 3, 4, 12, 17)	(3, 4, 15, 21, 22)	(3, 4, 9, 20, 23)
53127	(20, 21, 22, 23, 24)	(2, 3, 4, 7, 20)	(3, 4, 20, 21, 22)	(4, 15, 20, 21, 24)
53128	(15, 16, 17, 18, 19)	(2, 3, 4, 17, 20)	(3, 4, 18, 20, 21)	(3, 4, 9, 20, 24)
53129	(5, 6, 7, 8, 9)	(2, 3, 4, 12, 20)	(3, 4, 13, 20, 21)	(0, 3, 4, 9, 20)
53130	(10, 11, 12, 13, 14)	(2, 3, 4, 20, 21)	(3, 4, 8, 20, 21)	(0, 4, 15, 20, 21)

Table 3.6 - Power loss in percentage corresponding to the ranking with n = 5

Ranking	0 degrees	15 degrees	30 degrees	45 degrees
1	9.93%	18.50%	18.07%	11.83%
2	10.04%	18.50%	18.07%	11.84%
3	10.04%	18.50%	18.07%	11.84%
4	10.04%	18.50%	18.09%	12.02%
5	10.05%	18.50%	18.09%	12.02%
…				
53126	19.98%	20.52%	20.60%	22.39%
53127	19.98%	20.52%	20.60%	22.40%
53128	20.00%	20.52%	20.67%	22.40%
53129	20.01%	20.52%	20.67%	22.40%
53130	20.01%	20.52%	20.69%	22.40%

Maintenance Scheduling and AEP Calculation

The second scope FLORIS is used for is to schedule maintenance; thus calculate its associated downtime energy losses, and the AEP. In fact, while it is important to evaluate the impact that scheduling maintenance considering

wake effect has on energy losses, it is also crucial to assess its impact on the annual energy production, which is clearly closely related to the energy loss.

Therefore, firstly the energy production that would be guaranteed without ever performing maintenance is calculated for every year, that is the maximum AEP of the wind farm. The outcome is shown in Figure 3.16.

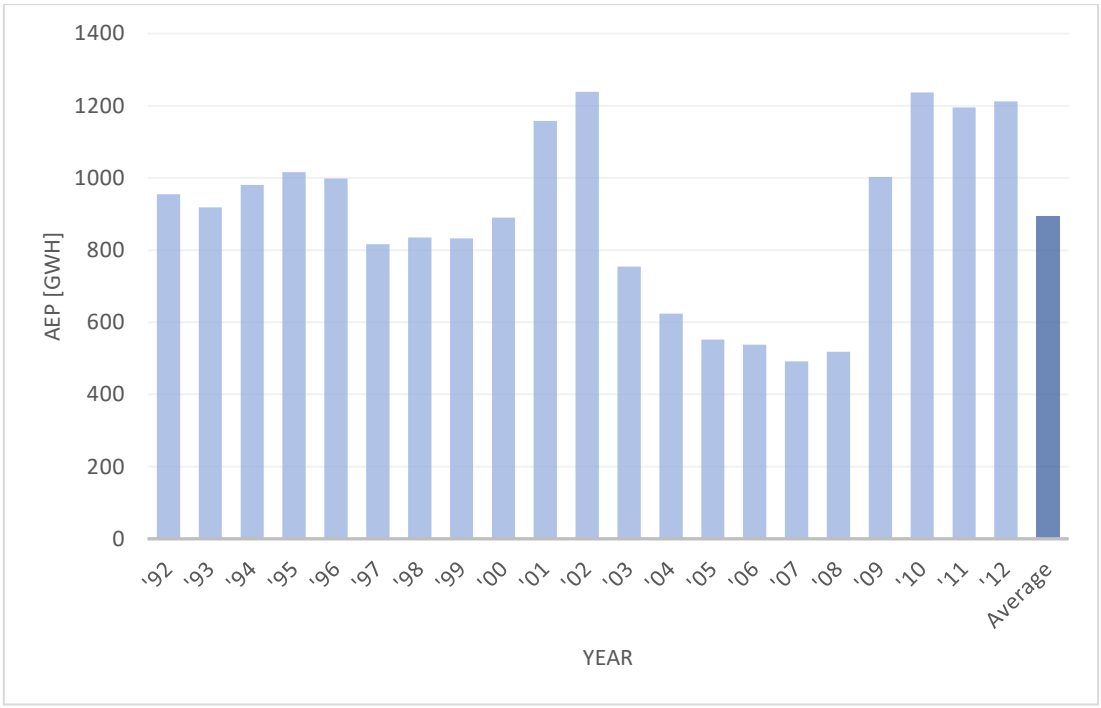

Figure 3.16 – Maximum AEP

Then, the maintenance activities are scheduled on a day-to-day basis, deciding on which turbines to operate based on the representative wind of each day. As the ranking of sets of turbines is computed with a resolution of five degrees, the closest value to the representative wind direction is used. To define the cases, four variables are considered, as displayed in Table 3.7. Maintenance is scheduled according to three methods:

- *Optimized Scheduling*: the maintenance plan is scheduled considering wake effect, in order to minimize the energy losses associated to it.
- *Sequential Scheduling*: the maintenance plan is scheduled ignoring wake effect, starting from the five southern-most turbines and moving up once a set of turbines has completed 80 hours of maintenance.
- *Worst Case Scheduling*: the maintenance plan is scheduled to maximize the downtime energy losses, to assess the difference between this and Optimized Scheduling.

Regular CTVs are only used for maintenance scheduled with a binary criterium, whereas Novel CTVs are used to plan maintenance both with binary and non-binary criteria. Optimized and Sequential scheduling are applied to all the mentioned cases (binary criterium with Regular CTVs, and binary and non-binary criteria with Novel CTVs), whereas the worst-case scheduling is only simulated for Regular CTVs. If not specified otherwise, maintenance is scheduled on sets of five turbines, due to the limitations of regular CTVs. Nevertheless, to assess the advantage of operating on more turbines at the same time, the non-binary criterium was also applied to schedule maintenance on sets of six turbines, with novel CTVs. The objective of the present work is to assess the impact of a non-binary decision strategy and considering wake effect on maintenance scheduling. Therefore, the Base Case, used as a reference to examine how it can be improved by this approach, is characterized by sequential scheduling, implemented through a binary criterium. Table 3.8 summarizes the cases that are simulated.

Table 3.7 - Variables for case definition

CTV Type	Regular	Novel	
Criterium	Binary	Non-Binary	
Size of set of turbines	5 T	6 T	
Scheduling logic	Optimized	Sequential	Worst case

Table 3.8 - Cases

Case	CTV Type	Criterium	n	Scheduling logic
Base Case – 0	Regular	Binary	5	Sequential
1	Regular	Binary	5	Optimized
2	Regular	Binary	5	Worst-case
3	Novel	Binary	5	Sequential
4	Novel	Binary	5	Optimized
5	Novel	Non-Binary	5	Sequential
6	Novel	Non-Binary	5	Optimized
7	Novel	Non-Binary	6	Optimized

The binary criterium implies that maintenance activities are scheduled whenever the weather conditions allow it, namely when the maximum significant wave height and wind speed during the day are lower than the thresholds imposed by the vessels, the significant wave height being the limiting factor. In fact, novel CTVs open more workable windows; hence it is possible to schedule maintenance with these vessels with a non-binary criterium. Namely, it is possible to impose stricter limitations on wind speed and operate when it is low; thus, reducing the energy loss due to downtime. Obviously, the decision on whether to work or not on a workable day can be more conservative or less depending on the turbines that are maintained at the same time. Hence, different criteria were implemented in the two cases analyzed: five turbines and six turbines. Figure 3.17 shows how the limit wind speed is chosen every day to decide whether to operate or not. For the first two months, the threshold U_{lim1} is manually defined, and it is equal to 3 m/s. In the following months, the limit wind speed depends on what percentage of maintenance has already been carried out: in June and July, the threshold is one third of the annually maintenance; in August it is two thirds of the total. The limit wind speed in these months depends on the size of the sets of turbines: if 5 turbines are maintained simultaneously, the limits are 4.5 m/s (U_{lim2}) and 5.5 m/s (U_{lim3}), respectively; if each set consists of 6 turbines, the limit is 4 m/s in June and July and 5 m/s in August. Finally, in September and October, when maintenance is completed the process is ended; otherwise, the limit wind speed (U_{lim4}) increases to 7 m/s and 6.5 m/s respectively for sets of five and six turbines.

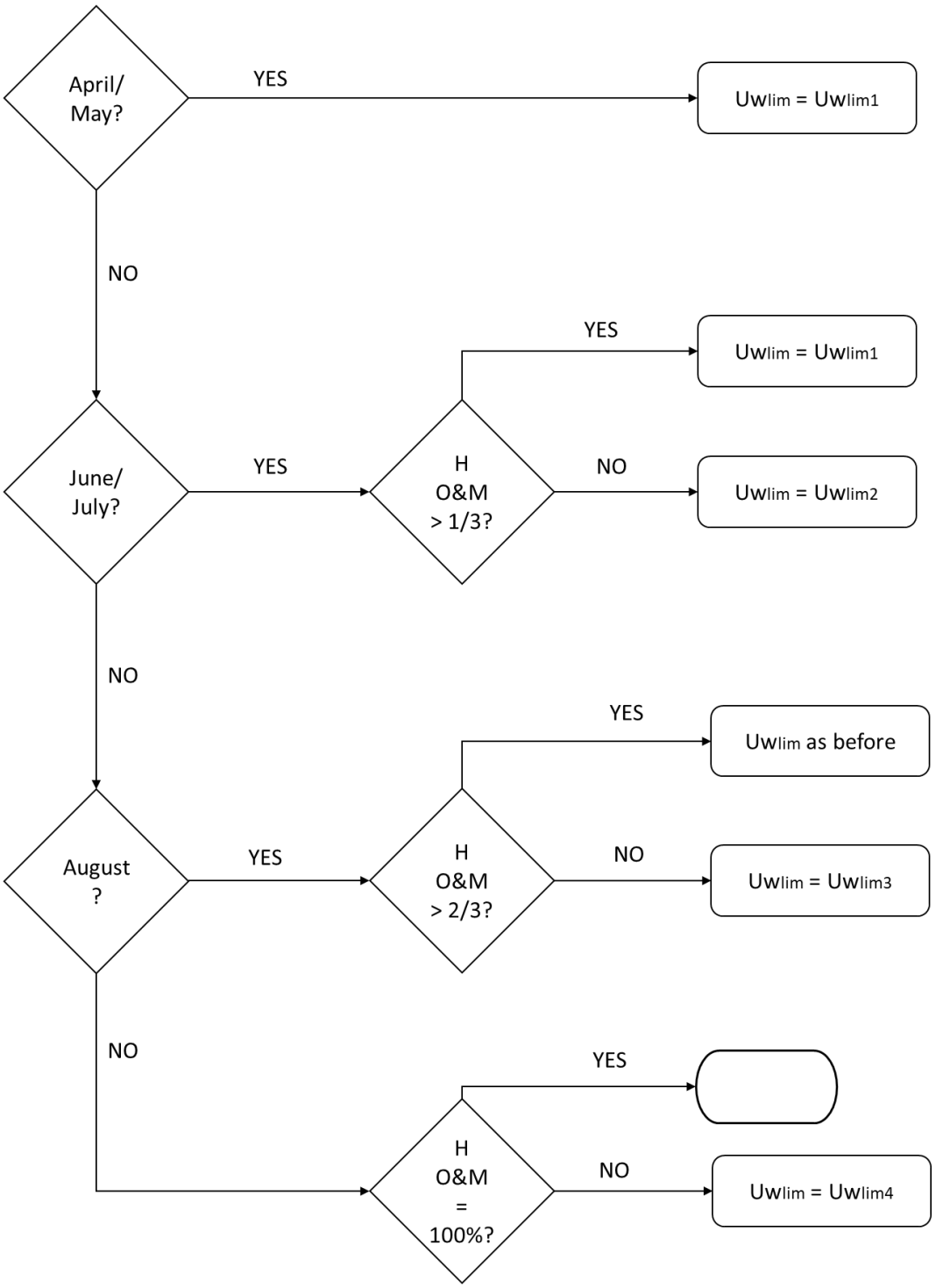

Figure 3.17 - Limit wind speed flowchart

Figure 3.18 and Figure 3.19 depict the procedure followed to plan maintenance with an optimized scheduling logic and with a sequential one, respectively. The procedure represented is valid both for binary and non-binary criteria. In case a binary criterium was used, U_{wlim} must be equal to the technical limitation of the CTV (15 m/s).

As opposed to this, with a non-binary criterium U_{wlim} is calculated as displayed in Figure 3.18 Once a year is over, the output DataFrame is stored in an Excel to be post processed.

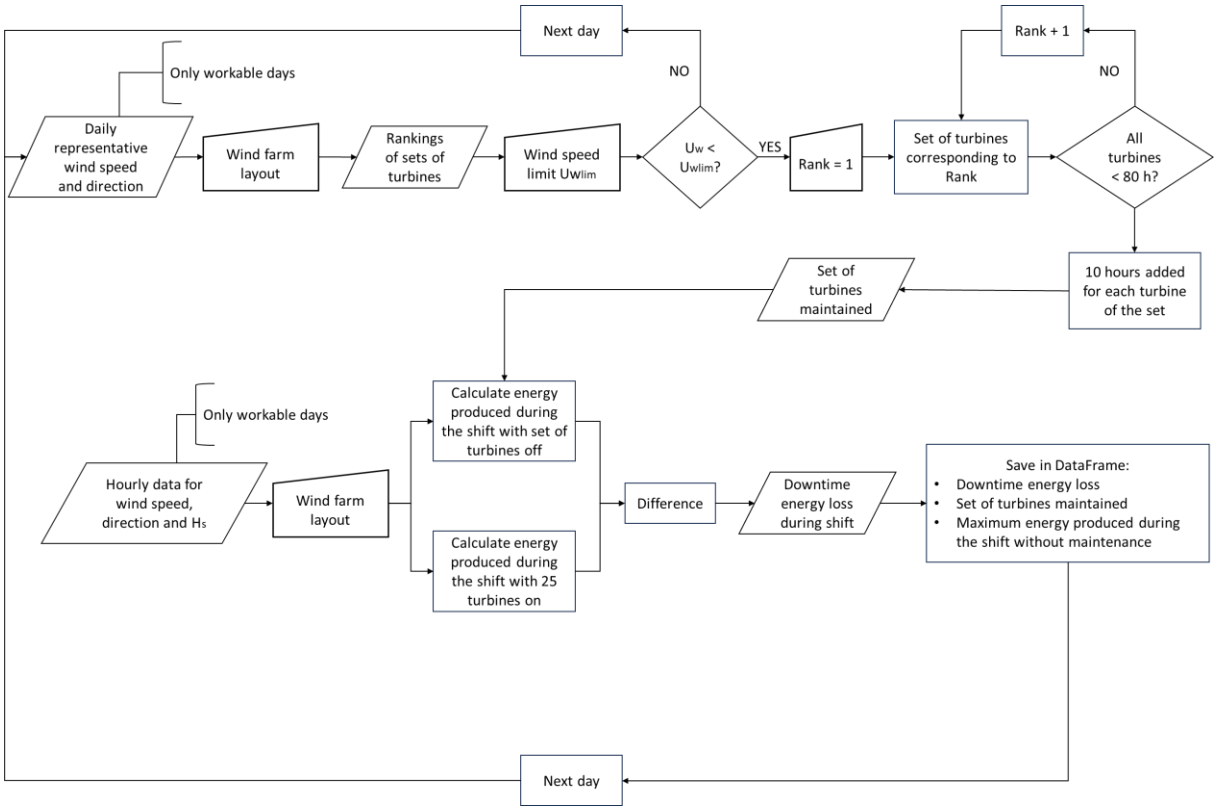

Figure 3.18 - Flowchart for Optimized Scheduling

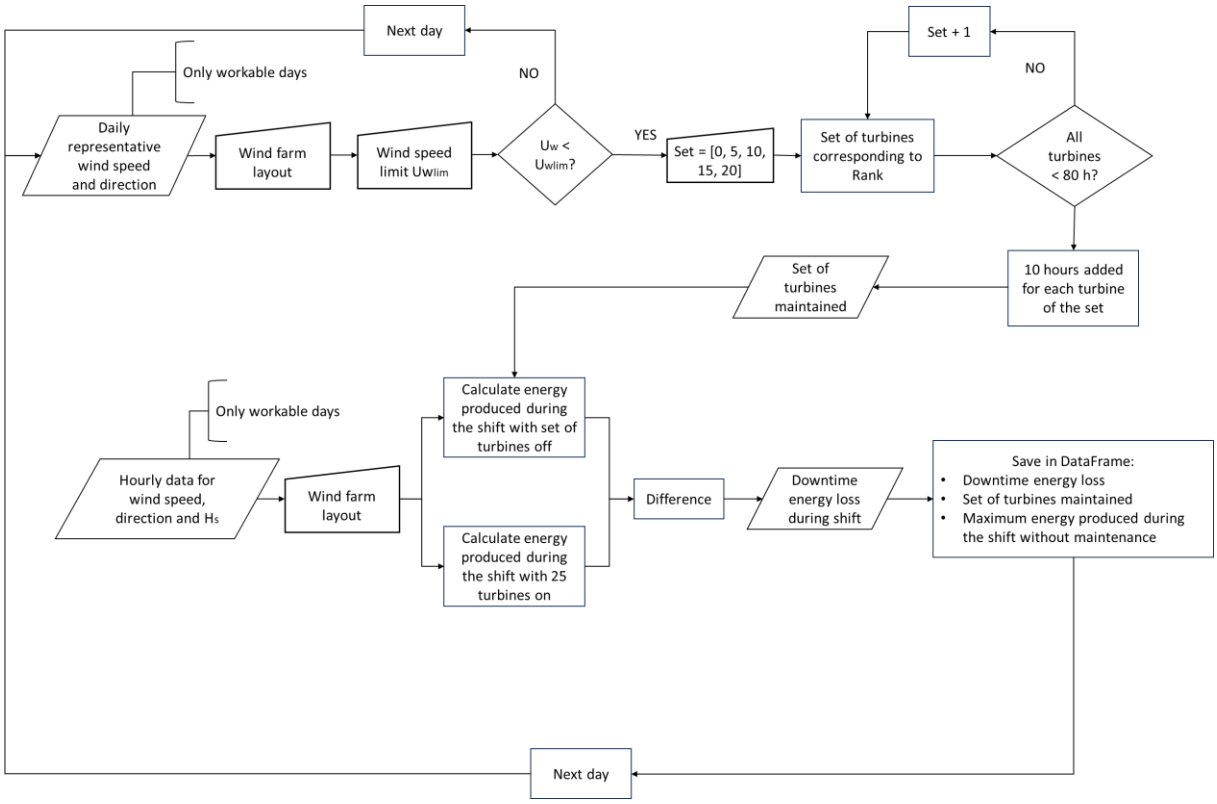

Figure 3.19 - Flowchart for Sequential Scheduling

Figure 3.20 compares the monthly average workable days with a binary criterium and with a non-binary criterium, maintaining 5 or 6 turbines simultaneously. The very strict conditions imposed for the first months cause the number of workable days to be significantly lower for the non-binary criterium. Nevertheless, the wider workable windows obtained thanks to Novel CTVs allows to have enough days to maintain all the turbines increasing the workable days later, if necessary.

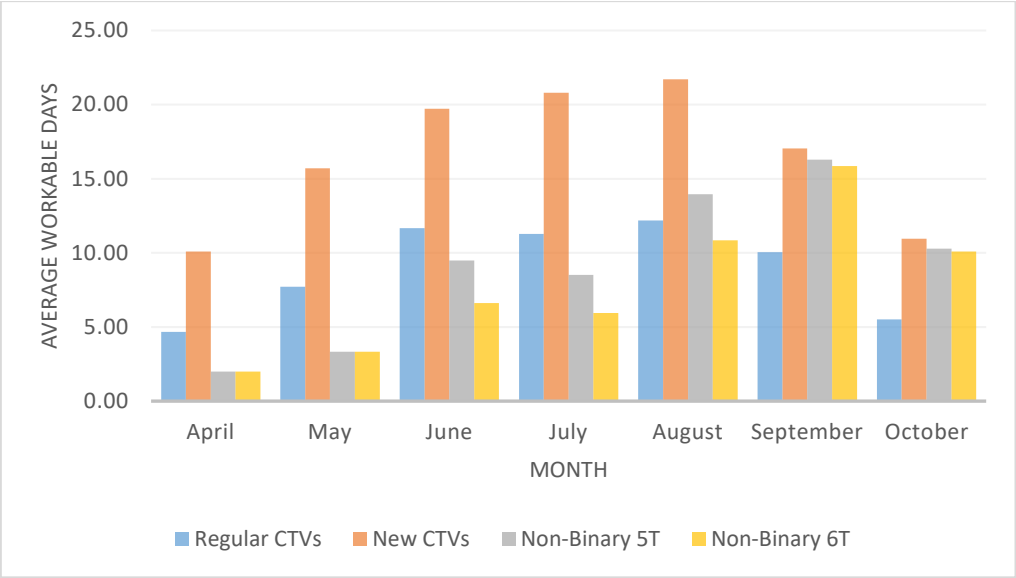

Figure 3.20 – Average Workable Days per month with Regular CTVs and Novel CTVs (Binary criterium) and with Non-Binary criterium

The set of turbines that undergo maintenance for a given day is defined entering a table analogous to the example in Table 3.5, but including all the wind directions and the complete ranking of all the possible sets. When the best set of turbines to maintain is chosen based on the representative wind direction, it is necessary to check if any of the turbines has already received 80 hours of maintenance. If this is the case, the second-best set is tried and so on, until a set of turbines who have not received the annual required maintenance is found. Concerning the worst-case scheduling, the procedure is the same but, instead of starting from the first set of turbines, it starts from the last. Finally, sequential maintenance is scheduled such that maintenance is performed firstly on the southern-most five turbines, and, when eight days of maintenance are carried out, it moves to the next set of turbines towards north. Therefore, the first set of turbines maintained is (T0, T5, T10, T15, T20) and the last one is (T4, T9, T14, T19, T24). When a set of turbines is maintained, 10 hours of maintenance are added to each of the turbines in a counter that keeps track of the hours of maintenance performed on every turbine.

Once it is decided if maintenance is carried out on the day and the set of turbines to be maintained is selected, the energy loss for the day is computed as the difference between the nominal energy production and the energy produced when the chosen set of turbines is switched off. When representative wind speed is used for the whole day, the energy loss is calculated multiplying the power loss by 10, which is the length of the maintenance operations; whereas when real data are used, the power loss is calculated for every hour and, as the data are hourly, the sum of the losses during the 10 hours is equal to the energy loss of the day. To examine how the representative wind speed and direction really represents the variations of wind conditions throughout the day, the real energy production and the downtime energy losses of workable days is compared to the representative energy production for every year in Figure 3.21. The figure shows that there is a difference, although relatively

small, between real and representative downtime losses. Worst-case Scheduling tends to overestimate the losses with representative wind conditions, as well as Sequential Scheduling. On the other hand, Optimized Scheduling presents very similar results for relatively low losses, whereas the error increases – be it overestimating or underestimating – for higher losses. Nevertheless, the representative wind conditions reflect the weather variation during the day, suggesting that the sets of turbines to maintain are well chosen.

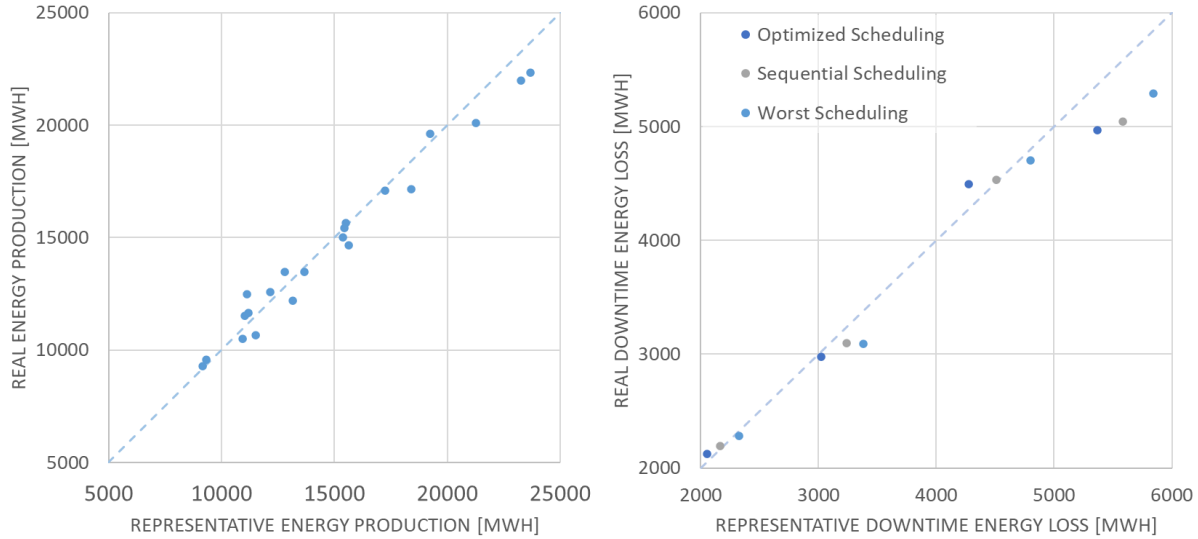

Figure 3.21 - Comparison of Real and Representative Energy Production on Workable Days [Left] and Comparison of energy losses due to downtime calculated with representative and hourly wind data in years (from left to right) 2011, 1998, 2010, 2002 [Right]. On dot corresponds to one year

4. Results

This chapter presents the results obtained in terms of reduction of energy loss, with a focus on evaluating the improvement given by considering the impact of wake effect with respect to implementing a sequential logic with a binary criterium to schedule maintenance, as this is considered the Base Case. It is of key importance to assess if considering wake effect to select the turbines to maintain leads to a significant decrease of downtime energy losses, especially compared to said Base Case.

4.1 Regular CTVs

Firstly, the results obtained with Regular CTVs are compared, to evaluate the decrease of downtime energy losses ensured by optimized scheduling, when compared to sequential scheduling as well as to the worst-case scheduling.

Figure 4.1 depicts the downtime energy losses for every year, with the three scheduling strategies. The first thing that can be noticed is that downtime losses vary significantly from one year to another. For further comparisons, namely with results obtained applying a non-binary criterium, it is important to highlight that in years 2011 and 2012 not all the turbines receive the hours of maintenance required. In fact, these two years only have 30 and 28 workable days respectively, whereas 40 days are needed to be able to complete maintenance on the whole wind farm. Therefore, in 2011 it is possible to carry out up to 1500 hours of maintenance, whereas in 2012 the weather conditions only allow 1400 hours of maintenance, out of the 2000 hours that would be needed. Not being able to complete the required maintenance leads to a higher risk of components failure. This can increase the losses significantly if a failure occurs, as the turbine needs to be shut down until the component is repaired or replaced, which might take several days if the weather conditions are too severe. Moreover, it is important to highlight the reduction in terms of downtime losses that is given by maintaining six turbines at the same time instead of five.

It can be expected that the optimized scheduling would lead to lower losses than sequential scheduling with the worst-case scheduling being, as the name suggests, the one that entails the highest energy loss. Figure 4.2 shows that the worst-case scheduling is always the strategy that causes the highest downtime losses. On the other hand, the expectations are not always met concerning the comparison between optimized and sequential scheduling: in 2003, the sequential scheduling turns out to be the one that entails the lowest energy loss. This can be explained by the fact that, even though downtime losses are calculated using hourly data for wind speed and direction, the set of turbines to maintain is selected based on the representative wind direction. Although the latter is calculated to consider that the wind direction can change significantly during a day, there can be some days in which its variation throughout the daylight hours is not well represented by the representative wind direction. This can result in having higher losses with optimized scheduling than with sequential scheduling. Figure 4.3 shows a comparison between real and representative downtime energy losses in 2003 for the three

scheduling logics. From the figure, it can be noticed that, while the Optimized Scheduling is very close to having the same result with representative and real data, Sequential Scheduling is overestimated with representative wind conditions. Therefore, the real downtime loss is lower than the representative one, which is why it is also lower than the loss that is entailed by Optimized Scheduling. Overall, scheduling maintenance considering the impact of wake effect has a positive outcome throughout the 21 years considered for the present work. In fact, it allows to reduce downtime losses on average by 2.27 % with respect to sequential scheduling and by 5.91 % with respect to worst-case scheduling, as shown in Table 4.1.

Table 4.1 - Average percentual improvement obtained by Optimized Scheduling with respect to Sequential and Worst-case Scheduling

	Percentual reduction of downtime energy losses
Sequential Scheduling	2.74 %
Worst-case Scheduling	6.26 %

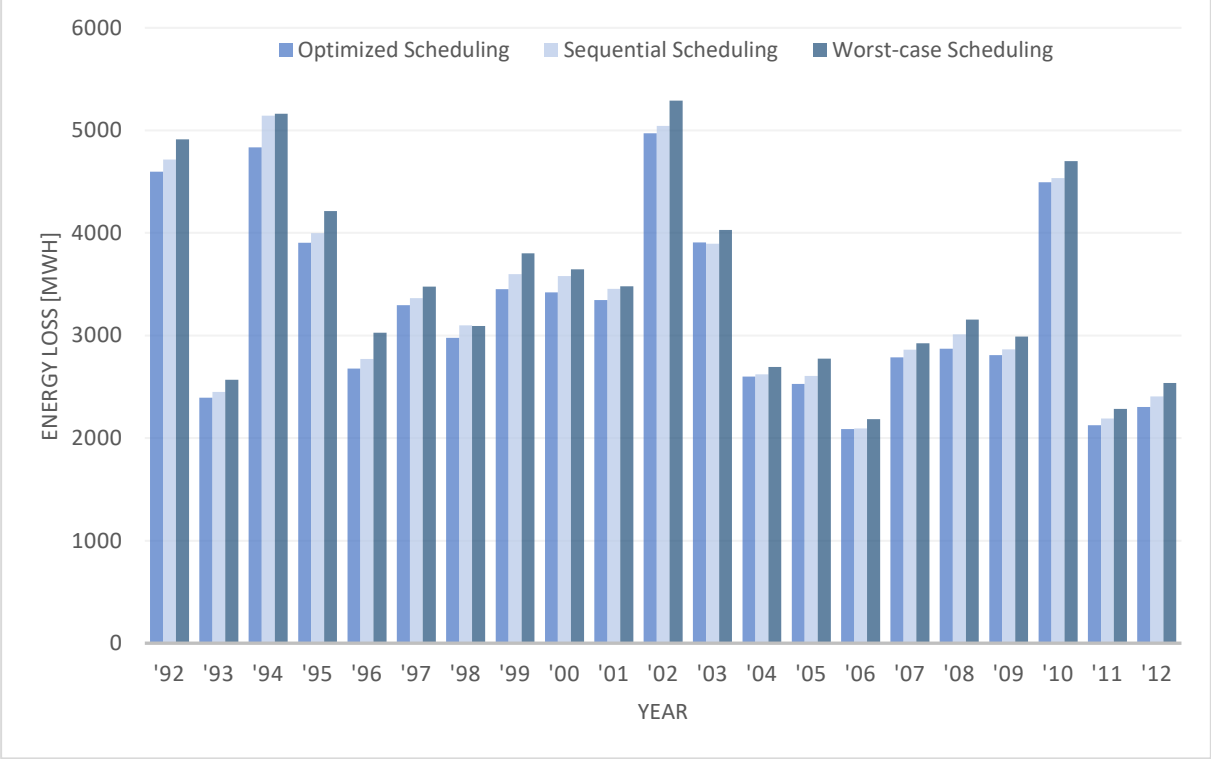

Figure 4.1 - Energy Losses due to downtime, calculated with hourly wind conditions for Regular CTVs

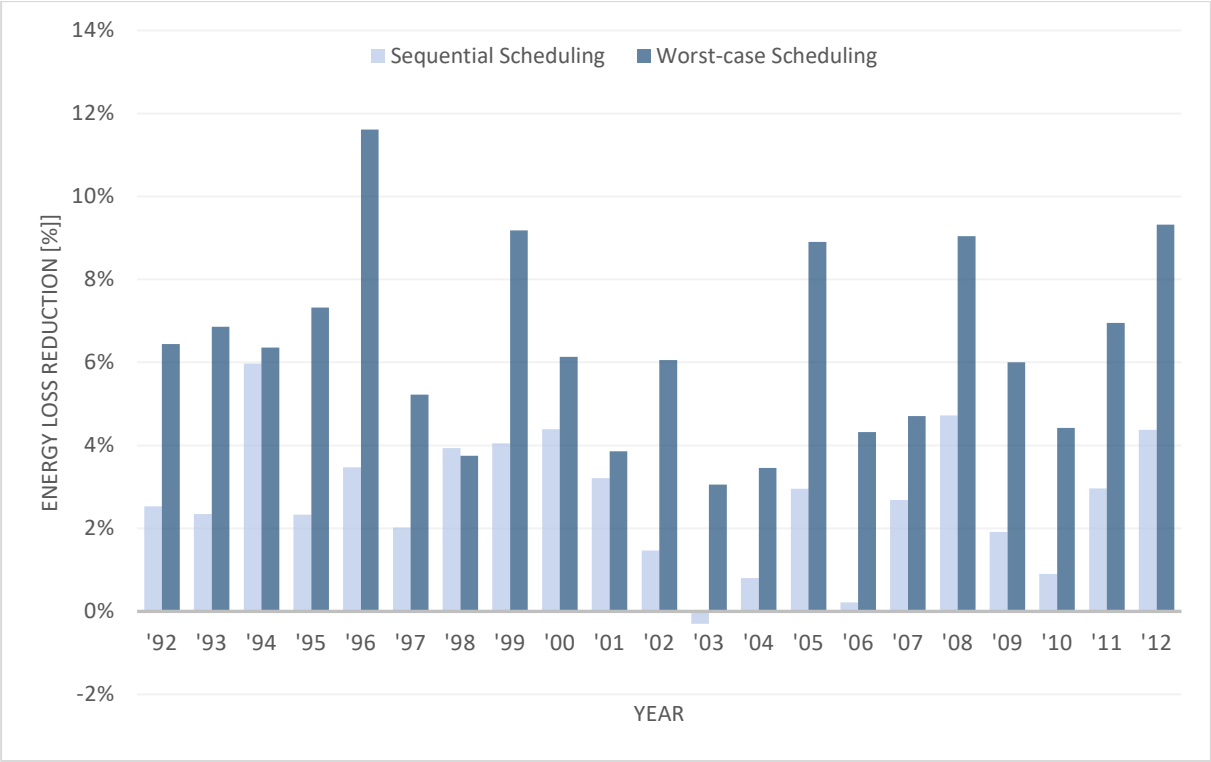

Figure 4.2 - Percentual Improvement thanks to Optimized Scheduling in comparison with Sequential and Worst Scheduling

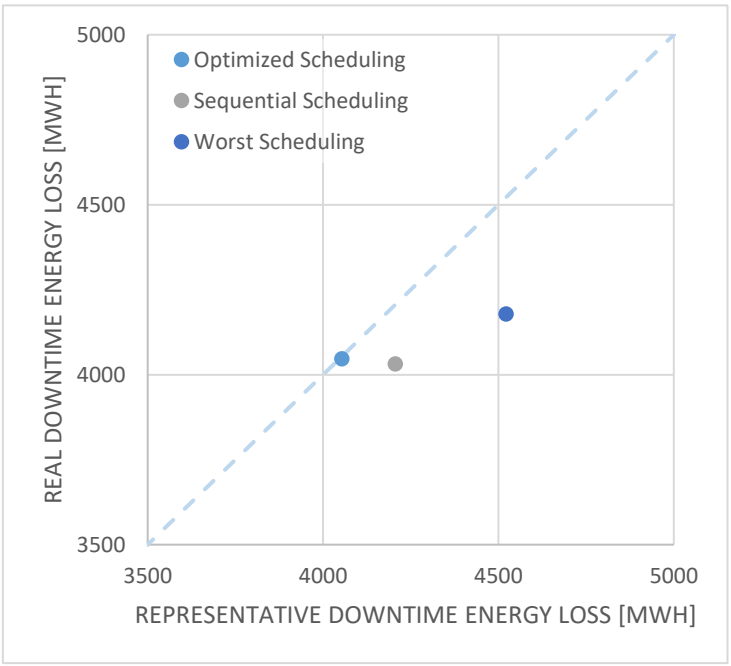

Figure 4.3 - Comparison of energy losses due to downtime calculated with representative and hourly wind data in year 2003

As explained in Weather Data Analysis, regular CTVs can only operate with significant wave heights up to 1.5 meters, which translates into a limited number of workable days. Consequently, it is imperative to carry out

maintenance whenever the significant wave height allows it, disregarding the wind speed. Because the latter is not the critical limiting factor, with a binary criterium, maintenance is performed when wind speed, measured at a 10 m height, is lower than 15 m/s. The rated wind speed is 10.59 m/s at hub height, or 8.47 m/s at 10 m height. Therefore, this approach is not optimal, as the turbines are maintained in days with high wind speed, hence entailing significative downtime energy losses.

For this reason, a new approach was implemented by means of using novel CTVs, that are capable to operate under harsher sea conditions, namely with significant wave height up to 2 m. Increasing this limitation opens several workable windows, thus allowing the development and implementation of a non-binary criterium.

4.2 Novel CTVs

Therefore, in this section the results obtained with novel CTVs are presented. At first, results obtained with a binary criterium are shown, then moving on to a non-binary criterium to furtherly reduce downtime energy losses.

Binary Criterium

Figure 4.4 depicts the downtime energy losses that occur when scheduling maintenance with a binary criterium over the workable windows available with Novel CTVs, comparing the results obtained with the ones that were obtained with Regular CTVs. As it happened with Regular CTVs, optimized scheduling ensures an improvement with respect to sequential scheduling throughout the whole period considered, with an average of 1.99 % decrease in yearly downtime energy loss. The exception to this is years 1996, 1998 and 2003, in which the sequential scheduling seems to be the best solution. The cause can be attributed, analogously to the case of Regular CTVs, to the fact that the set of turbines to maintain is selected based on the representative wind direction, whereas during the day this parameter can vary.

For both optimized and sequential scheduling, downtime losses are significantly higher than the ones occurring with Regular CTVs. This is because increasing the limit significant wave height increases the workable days that are available. Therefore, with a binary criterium that imposes to perform maintenance whenever a workable day occurs, most of the activities are carried out during spring, as displayed in Figure 4.6. Spring is characterized by higher wind speeds than summer, thus maintaining the turbines during this season entails higher downtime losses. Years 1997, 2007 and 2008 are an exception, as applying the binary criterium with Novel CTVs decreases the downtime energy losses, compared to the same criterium applied with Regular CTVs.

Finally, the figure shows a wider difference between the results obtained with the two types of CTVs in year 2011 and 2012, compared to previous years. In these two years, with Regular CTVs it was not possible to complete all

the required hours of maintenance, as mentioned above. On the other hand, Novel CTVs make it possible to complete 2000 hours of maintenance on every turbine, thus entailing higher downtime losses.

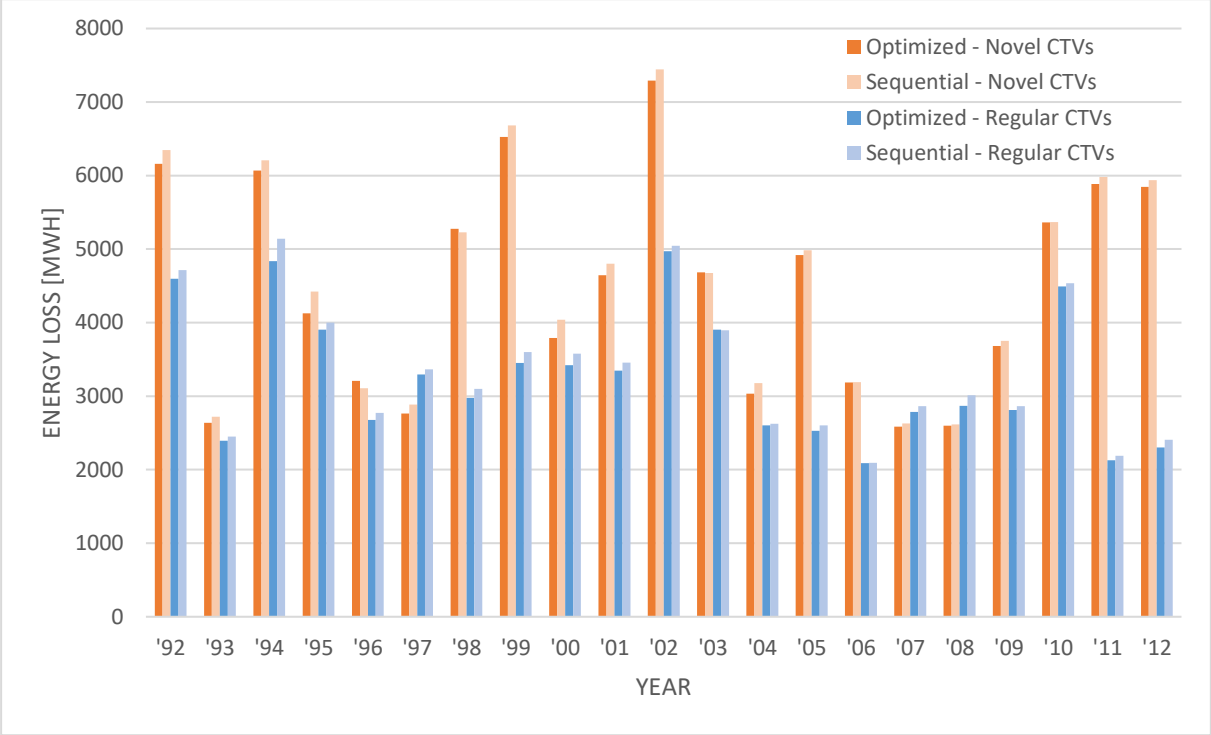

Figure 4.4 – Downtime energy losses, comparison between Novel and Regular CTVs

Non-Binary Criterium

The Non-Binary Criterium is applied to Sequential Scheduling and Optimized Scheduling. For the former, only the possibility of maintaining 5 turbines simultaneously is considered, whereas for the latter simulations are run for sets of 5 and 6 turbines maintained at the same time. Figure 4.5 displays the downtime energy losses by year, in the three cases analyzed, comparing them with the Base Case. The first thing that can be noticed, and is can seem unexpected, is that in 2011 and 2012 the Base Case seems to be the one that entails the least losses. Nevertheless, this is because Regular CTVs do not guarantee enough workable days to complete the maintenance planned, required by every turbine, hence the energy losses seem to be lower. This can lead to a higher risk of failure, and thus prolonged downtime periods, as mentioned above. Moreover, in 2009 sequential scheduling with Regular CTVs entails lower downtime energy losses than maintenance planning with a non-binary criterium on sets of 5 turbines. In said year, the wind conditions only allow a small number of workable days in spring and maintenance spills into September, whereas in other years it is completed by the end of August or mid-September at the latest. Consequently, the wind speed thresholds need to be less conservative, to be able to carry out the hours of maintenance required, thus causing higher downtime losses. There are other years

(namely, 1999, 2002 and 2010) in which maintenance activities continue until the end of September or even until October. These years are 1999, 2002 and 2010, although in 1999 wind speeds are low during Fall; thus, downtime losses are not influenced by the fact that maintenance is carried out until October. On the other hand, in 2002 and 2010 downtime energy losses are remarkably high. Nevertheless, the Base Case entails even higher losses, making the non-binary criterium the most convenient solution, despite entailing higher downtime losses than in the other years.

The results obtained over the 21 years are summarized in Table 4.2, highlighting the overall great advantages given by imposing stricter wind speed thresholds to perform maintenance. Sequential scheduling applied with a non-binary criterium, thanks to novel CTVs, already reduces downtime losses significantly throughout the 21 years, with respect to the Base Case. Nevertheless, if the non-binary criterium is applied to minimize downtime losses caused by wake effect (optimized scheduling), it is possible to reduce the energy losses by up to 48.2 % with respect to the Base Case if 6 turbines are maintained simultaneously, or by 36.5 % if operating on sets of 5 turbines.

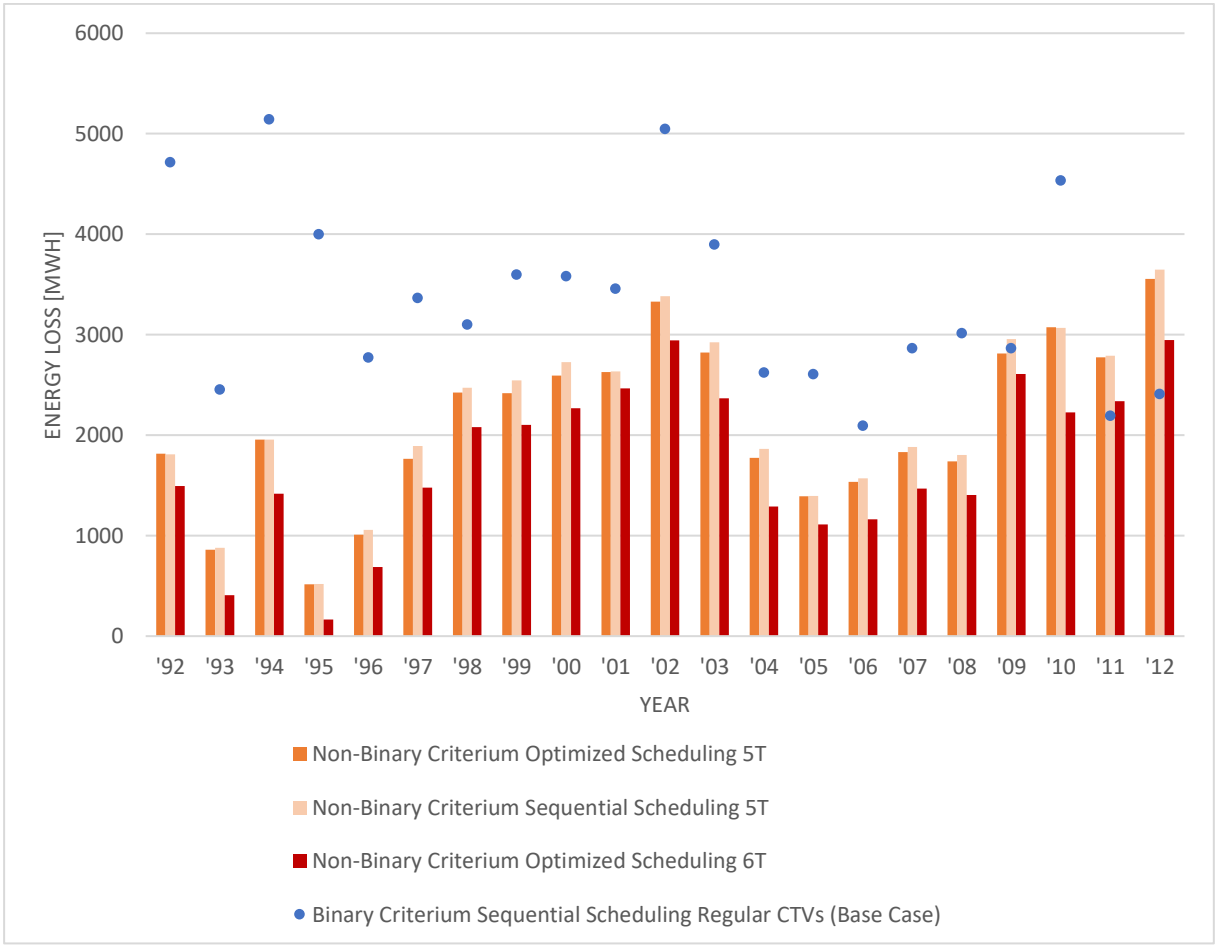

Figure 4.5 - Energy Losses due to downtime, Non-Binary Criterium with sets of 5 turbines (5T) and 6 turbines (6T) compared with Base Case (Sequential Scheduling with Binary Criterium)

Table 4.2 – Downtime energy losses. Non-Binary Criterium with sets of 5 turbines (5T) and 6 turbines (6T) compared with Base Case (Sequential Scheduling with Binary Criterium)

	Base Case	Sequential 5T, Non-Binary	Optimized 5T, Non-Binary	Optimized 6T, Non-Binary
Total Energy Loss [MWh]	70311.0	45770.4	44625.6	36438.6
Percentual Improvement	-	34.9 %	36.5 %	48.2 %

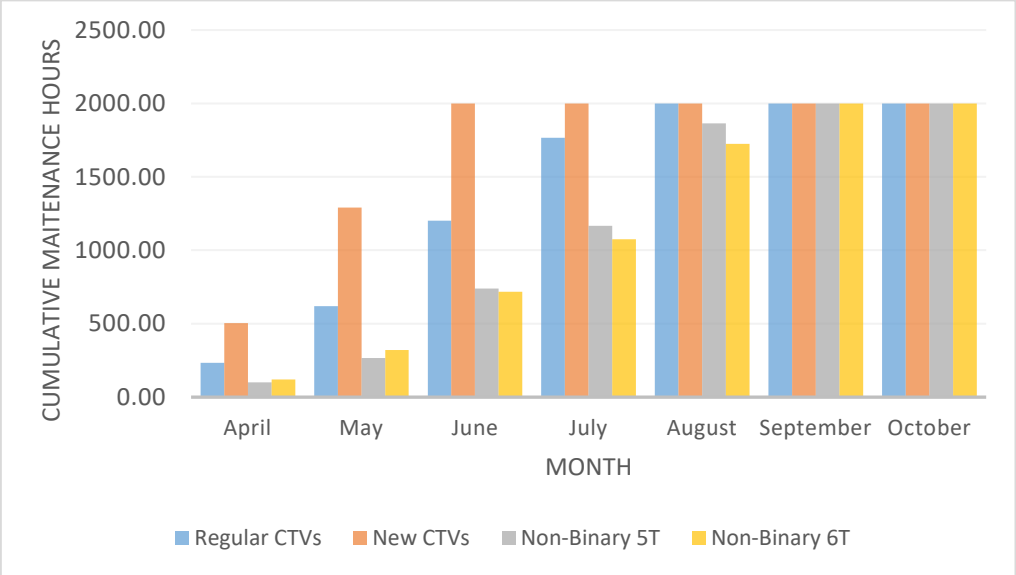

Figure 4.6 – Average cumulative hours of maintenance for the cases studied

4.3 Annual Energy Production

Finally, the AEP is calculated over the whole period, with hourly data for wind speed and direction, to assess the impact of the maintenance strategies that were implemented on the energy produced. The average AEP, without considering downtime losses, is equal to 893.57 GWh; thus, the CF is 27.2 %. This is due to the fact that non-valid timestamps are present in the weather data, and thus it was not possible to calculate the exact power production in those timeframes.

Table 4.3 summarizes the results obtained, showing that implementing a maintenance strategy following a non-binary criterium can increase the AEP by 0.14 % if operating on sets of five turbines and by 0.18 % if six turbines

are maintained at the same time. These numbers might seem small, but they translate in, respectively, 117 and 161 households supplied per year, as one household consumes around 10 MWh of electricity per year [71].

Table 4.3 - Comparison with Sequential Maintenance (Binary Criterium) with Regular CTVs

	Optimized, Regular CTVs	Optimized Binary New CTVs	Optimized 5T, Non-Binary	Sequential 5T, Non-Binary	Optimized 6T, Non-Binary
Energy Loss [%]	-2.74 %	34.09 %	-36.53 %	-34.90 %	-48.18 %
AEP [%]	0.01 %	-0.13 %	0.14 %	0.13 %	0.18 %
Households	9	-114	122	117	**161**

Therefore, this approach is proved to reduce significantly the downtime energy losses that are associated with preventive maintenance, by operating on three aspects: considering wake effects to schedule activities, the type of CTV, and the possibility to operate only below a certain wind speed. All these variables have an impact on the outcome, although the most significant improvement is obtained by using a non-binary criterium, as opposed to the binary one. Nevertheless, the possibility to implement such a criterium solely depends on the choice of CTVs, in this location. In fact, without the use of novel CTVs, it would have not been possible to have enough workable days available to apply a non-binary criterium based on wind speed. Finally, wake effects have an impact, as optimized scheduling entails less downtime losses than sequential scheduling, but the reduction is not as significant as the one obtained thanks to the non-binary criterium. Combining all these factors allowed to schedule a preventive maintenance plan that significantly reduces the downtime losses compared to the base case of planning sequential scheduling, with regular CTVs and binary criterium.

5. Conclusion

The present work was able to identify the main limiting factor in preventive maintenance scheduling and find a solution to loosen such constraint, to obtain an improvement of performances. Namely, downtime energy losses were significantly reduced.

The last chapter draws conclusions from the results obtained and aims to suggest the next steps that could contribute to an even better maintenance planning. The development of the present thesis, as mentioned, builds up on previous work and is expected to be followed by future steps, to further improve the results obtained and add ulterior considerations. It was possible to improve the results, compared to the previous work, mostly thanks to the fact that the method to calculate the representative wind direction was changed and that Novel CTVs were contemplated. This increased the number of workable days, hence allowing a more conservative strategy to only carry out maintenance at low wind speed. This strategy was demonstrated to be able to significantly reduce downtime energy losses with respect to a binary criterium, according to which maintenance is carried out whenever the significant wave height allows it, hence operating at high wind speeds causing significant losses.

5.1 Main Findings

The results obtained suggest that wake effect is an important aspect to be considered in maintenance planning, as the aerodynamic interactions between turbines can be exploited to reduce downtime energy losses by operating on those turbines that, under certain wind conditions, maximize the energy production if switched off. The main findings of the present work are the following:

- The representative wind direction describes how the wind conditions change throughout the day in a more realistic way than the mean value, which was used in previous studies. Consequently, the downtime energy losses obtained with the present method are lower than the ones obtained in the mentioned previous study.
- The fact that in some years the Sequential Scheduling seems to be the best solution, entailing less downtime losses than the Optimized Scheduling, suggests that the calculation of the representative wind direction could be further improved. The representative wind direction is the only parameter considered to select the set of turbines to maintain; hence, the fact that the Optimized Scheduling is not the best solution suggests that there could be an improvement in the way this parameter is calculated. The strong variability of wind direction makes it difficult to calculate a representative value that describes in detail the variations that occur during the day.
- A non-binary approach that allows to exploit low wind days to perform maintenance can guarantee a significant improvement with respect to a binary criterium.
- In locations with severe weather conditions like the Atlantic Ocean, a significant wave height of 1.5 meters is too strict of a limitation to be able to implement such strategy. Lately, the industry has

developed bigger CTVs that can withstand significant wave heights up to 2 meters, entailing a much larger number of workable days. These vessels can also transport more technicians, hence more turbines can be maintained simultaneously by only using one CTV. In this work, a simulation was done with sets of six turbines, already showing a significant improvement.

5.2 Future Development

Future work could deepen the topic of the advantages given by maintaining even more turbines at the same time. On the other hand, five or six turbines out of twenty-five is already one fifth of the farm, or more. Therefore, if the same ratio is applied to bigger farms, more turbines would be maintained simultaneously and a similar result can be expected.

A wind farm with a nominal capacity of 375 MW is relatively small, if compared to the average European offshore wind farms size which is equal to 788 MW [72]. Therefore, it would be interesting to apply wake effect modelling to optimize the maintenance planning of a bigger wind farm, as well as considering a different layout than the squared one. Also, a different location might be to evaluate how the parameters of the model need to be changed to satisfy the requirements of a different geographical area. Some areas like Northern Spain (Galicia, Asturias, Basque Country), Western France (Aquitaine, Loire, Brittany) can be expected to have similar weather conditions, hence it is realistic that this model could obtain good results, without significant changes. On the other hand, areas like the North Sea and the Baltic Sea, or the Mediterranean Sea are characterized by different weather conditions, hence more changes can be expected to be required. Also, the use of forecasting weather conditions could be compared to hindcasting, as in the present thesis it was assumed that the hindcast is completely reliable, while in reality there is a margin of error in forecasting.

Moreover, in the future the time that the CTV requires to go from one turbine to another should be considered in a more precise way. For the present thesis, it was assumed that all the turbines start the maintenance shift at the same time. In reality, they do not, as after dropping the technicians at one turbine the CTV needs to navigate until the next one before the shift can start for the latter.

Finally, an economic evaluation on these novel CTVs should be conducted, to assess whether the reduction obtained in terms of downtime energy losses is enough to compensate the price of such CTVs, which are expected to be more expensive than regular ones. Sticking to the economic point of view, it would be of great importance to further develop the present work, by calculating the LCOE, to evaluate if it is competitive with other energy sources, traditional and renewable.

Bibliography

[1] BloombergNEF Offshore Wind Forecast, "Global Offshore Wind Report 2022," World Forum Offshore Wind, 2023.

[2] IRENA, "Renewable Power Generation Costs in 2021," International Renewable Energy Agency, Abu Dhabi, 2022.

[3] M. Shafiee, "A fuzzy analytic network process model to mitigate the risks associated with offshore wind farms," *Expert Systems with Applications,* vol. 42, no. 4, pp. 2143-2152, 2015.

[4] Z. Ren, A. S. Verma, Y. Li, J. J. Teuwen and Z. Jiang, "Offshore wind turbine operations and maintenance: A state-of-the-art review," *Renewable and Sustainable Energy Reviews,* vol. 144, 2021.

[5] H. Seyr and M. Muskulus, "Decision Support Models for Operations and Maintenance for Offshore Wind Farms: A Review," *Applied Sciences,* vol. 9, no. 278, 2019.

[6] F. X. Correia da Fonseca, L. Amaral and P. Chainho, "A Decision Support Tool for Long-Term Planning of Marine Operations in Ocean Energy Projects," *Journal of Marine Sciende and Engineering,* vol. 9, no. 810, 2021.

[7] Vestas, "V236-15.0 MW™," Vestas, [Online]. Available: https://www.vestas.com/en/products/offshore/V236-15MW. [Accessed 05 May 2023].

[8] A. Memija, "Vestas 15 MW Prototype Turbine Produces First Power," offshoreWIND.biz, 30 December 2022. [Online]. Available: https://www.offshorewind.biz/2022/12/30/vestas-15-mw-prototype-turbine-produces-first-power/. [Accessed 05 May 2023].

[9] D. Snieckus, "'New global milestone' | China's CSSC Haizhuang rolls out world's largest wind turbine," Recharge, 06 January 2023. [Online]. Available: https://www.rechargenews.com/wind/new-global-milestone-chinas-cssc-haizhuang-rolls-out-worlds-largest-wind-turbine/2-1-1384424. [Accessed 05 May 2023].

[10] A. Lee, "Huge 'world first' zero-subsidy floating wind farm with 20MW turbines planned off Portugal," Recharge, 17 October 2022. [Online]. Available: https://www.rechargenews.com/wind/huge-world-first-zero-subsidy-floating-wind-farm-with-20mw-turbines-planned-off-portugal/2-1-1335670. [Accessed 05 May 2023].

[11] M. Keene, "Comparing offshore wind turbine foundations," Wind Power Engineering, 4 January 2021. [Online]. Available: https://www.windpowerengineering.com/comparing-offshore-wind-turbine-foundations/. [Accessed 11 April 2023].

[12] Equinor, "Hywind Tampen: the world's first renewable power for offshore oil and gas," Equinor, [Online]. Available: https://www.equinor.com/energy/hywind-tampen. [Accessed 04 September 2023].

[13] M. Barooni, T. Ashuri, D. Velioglu Sogut, S. Wood and S. Ghaderpour Taleghani, "Floating Offshore Wind Turbines: Current Status and Future Prospects," *Energies 2023,* 2022.

[14] Ghost456, "Offshore Wind Power," Wikipedia, 08 April 2022. [Online]. Available: https://en.m.wikipedia.org/wiki/File:Offshore_wind_foundation_types.svg. [Accessed 21 September 2023].

[15] Corrosion, "ICCP for floating devices," [Online]. Available: https://www.corrosion.nl/iccp-floating/. [Accessed 21 September 2023].

[16] J. McMorland, M. Collu, D. McMillan and J. Carrol, "Operation and maintenance for floating wind turbines: A review," *Renewable and Sustainable Energy Reviews,* vol. 163, 2022.

[17] Ørsted, "Making green energy affordable," Ørsted A/S, [Online]. Available: https://orsted.com/-/media/www/docs/corp/com/explore/making-green-energy-affordable-june-2019.pdf. [Accessed 05 May 2023].

[18] European Observation Network Territorial Development and Cohesion, "North Sea Regional Profile (Annex 7)," EU, 2013.

[19] Equinor, "The world's largest floating offshore wind farm officially opened," Equinor, 23 August 2023. [Online]. Available: https://www.equinor.com/news/20230823-hywind-tampen-officially-opened. [Accessed 20 September 2023].

[20] EniScuola, "The first turbine of Italy's first offshore wind farm, Beleolico, has been installed," Eni, 08 February 2022. [Online]. Available: https://eniscuola.eni.com/it-IT/news/2022/costruita-la-prima-turbina-di-beleolico-il-primo-impianto-eolico-offshore-ditalia.html. [Accessed 20 September 2023].

[21] Principle Power, "WindFloat Atlantic," [Online]. Available: https://www.principlepower.com/projects/windfloat-atlantic. [Accessed 20 September 2023].

[22] Principle Power, "Kincardine Offshore Wind Farm," [Online]. Available: https://www.principlepower.com/projects/kincardine-offshore-wind-farm. [Accessed 20 September 2023].

[23] Wind Europe, "Floating wind is making great strides," 12 May 2023. [Online]. Available: https://windeurope.org/newsroom/news/floating-wind-is-making-great-strides/. [Accessed 20 September 2023].

[24] Equinor, "Hywind Scotland," [Online]. Available: https://www.equinor.com/energy/hywind-scotland. [Accessed 20 September 2023].

[25] Principle Power, "Les Eolienne Flottantes du Golfe du Lion," [Online]. Available: https://www.principlepower.com/projects/les-eoliennes-flottantes-du-golfe-du-lion. [Accessed 20 September 2023].

[26] BW Ideol, "A Pre-Commercial Project of 3 units: EOLMED Project," [Online]. Available: https://www.bw-ideol.com/en/eolmed-project. [Accessed 20 September 2023].

[27] Provence Grand Large, "Provence Grand Large prend le large," 13 September 2023. [Online]. Available: https://provencegrandlarge.fr/le-projet/presentation-du-projet/. [Accessed 20 September 2023].

[28] "Floating Offshore Wind in Norway, TetraSpar Demonstrator," [Online]. Available: https://www.rwe.com/en/our-energy/discover-renewables/floating-offshore-wind/tetraspar/. [Accessed 20 September 2023].

[29] BW Ideol, " France's first offshore wind turbine and BW Ideol's first unit Floatgen," [Online]. Available: https://www.bw-ideol.com/en/floatgen-demonstrator. [Accessed 20 September 2023].

[30] RWE, "Floating Offshore Wind in Spain, DemoSATH," [Online]. Available: https://www.rwe.com/en/our-energy/discover-renewables/floating-offshore-wind/demosath/. [Accessed 20 September 2023].

[31] X1 Wind, "PivotBuoy Project: part-scale prototype in the Canary Islands," [Online]. Available: https://www.x1wind.com/projects/pivotbuoy-project-part-scale-prototype-in-the-canary-islands/. [Accessed 20 September 2023].

[32] M. Huleihil and G. Mazor, Wind Turbine Power: The Betz Limit and Beyond, 2012.

[33] NREL, "Offshore/IEA_15MW_240_RWT.csv," NREL/Github, 2020. [Online]. Available: https://github.com/NREL/turbine-models/blob/master/Offshore/IEA_15MW_240_RWT.csv. [Accessed 14 September 2023].

[34] M. de Prada Gil, O. Gomis-Bellmunt, A. Sumper and J. Bergas-Jané, "Power generation efficiency analysis of offshore wind farms connected to a SLPC (single large power converter) operated with variable frequencies considering wake effects," *Energy,* vol. 37, no. 1, pp. 455-468, 2012.

[35] R. B. S. Pereira, "Wind Farm Modelling," in *Lecture notes from the Wind Energy course held at Instituto Superior Técnico (Universidade de Lisboa)*, Lisbon, 2022.

[36] F. Gonzalez-Logatt, P. Wall and V. Terzija, "Wake effect in wind farm performance: Steady-state and dynamic behavior," *Renewable Energy,* vol. 39, no. 1, pp. 329-338, 2012.

[37] L. García, M. Vatn, F. Mühle and L. Sætran, "Experiments in the wind turbine far wake for the evaluation of an analytical wake model," *Journal of Physics: Conference Series,* vol. 854, 2017.

[38] M. Gaumond, P.-E. Réthoré, S. Ott, A. Peña, A. Bechmann and K. S. Hansen, "Evaluation of the wind direction uncertainty and its," *Wind Energy,* vol. 17, pp. 1169-1178, 2014.

[39] M. Bastankhah and F. Porté-Agel, "A new analytical model for wind-turbine wakes," *Renewable Energy,* vol. 70, pp. 116-123, 2014.

[40] T. Duc, O. Coupiac, N. Girard, G. Giebel and T. Göçmen, "Local turbulence parameterization improves the Jensen wake model and its implementation for power optimization of an operating wind farm," *Wind Energy Science,* vol. 4, no. 2, pp. 287-302, 2019.

[41] M. K. e. al., "Evaluation of Gaussian wake models under different atmospheric stability conditions: Comparison with large eddy simulation results," *Journal of Physics: Conference Series,* vol. 1669, 2020.

[42] A. Crespo and J. Hernández, "Turbulence characteristics in wind-turbine wakes," *Journal of Wind Engineering and Industrial Aerodynamics,* vol. 61, pp. 71-85, 1996.

[43] I. Katic, J. Højstrup and N. O. Jensen, "A Simpre Model for Cluster Efficiency," *W. Palz, & E. Sesto (Eds.), EWEC'86. Proceedings,* vol. 1, pp. 407-410, 1987.

[44] J. Annoni, P. Fleming, A. Scholbrock, J. Roadman, S. Dann, C. Adcock, F. Porte-Agel, S. Raach, F. Haizmann and D. Schlipf, "Analysis of control-oriented wake modeling tools using lidar field results," *Wind Energy Science,* vol. 3, no. 2, pp. 819-831, 2018.

[45] National Renewable Energy Laboratory, "FLORIS: FLOw Redirection and Induction in Steady State," NREL, [Online]. Available: https://www.nrel.gov/wind/floris.html. [Accessed 16 May 2023].

[46] C. Bay, J. King, P. Fleming, L. Martínez-Tossas, R. Mudafort, E. Simley and M. Lawson, "FLORIS: A Brief Tutorial," in *5th Wind Energy Systems Engineering Workshop*, Pamplona, 2019.

[47] P. Fleming, J. King, C. Bay, E. Simley, R. Mudafort, N. Hamilton, A. Farrell and L. Martínez-Tossas, "Overview of FLORIS updates," in *Journal of Physics: Conference Series*, 2020.

[48] R. B. S. Pereira, "Lecture 3 - Wind Climate pt. 2," in *Lecture notes from the Offshore Wind Energy course held at Instituto Superior Técnico (Universidade de Lisboa)*, Lisbon, 2022.

[49] G. van Bussel and M. B. Zaaijer, "Reliability, Availability and Maintenance aspects of large-scale offshore wind farms, a concepts study," in *MAREC 2001 Marine Renewable Energies Conference*, Newcastle, 2001.

[50] C. Zhu and Y. Li, "Reliability Analysis of Wind Turbines," 10 October 2018. [Online]. Available: https://www.intechopen.com/chapters/59756. [Accessed 08 May 2023].

[51] M. A. Lundteigen and M. Rausand, "Failures and failure classificiation," NTNU, Trondheim.

[52] J. Phillips, O. Fitch-Roy, P. Reynolds and P. Gardner, "A guide to UK offshore wind operations and maintenance," 2013.

[53] I. Bayati and L. Efthimiou, "Onsite Major Component Replacement Technologies for Floating Offshore Wind: the Status of the Industry," World Forum Offshore Wind e.V., 2023.

[54] A. Karyotakis, "On the Optimisation of Operation and Maintenance Strategies for Offshore Wind Farms. PhD Thesis," University College of London, London, 2011.

[55] P. J. Tavner, Offshore Wind Turbines: Reliability, availability and maintenance, 2012.

[56] S. Zhong, A. Pantelous, M. Goh and J. Zhou, "A reliability-and-cost-based fuzzy approach to optimize preventive maintenance scheduling for offshore wind farms," *Mechanical Systems and Signal Processing,* vol. 124, pp. 643-663, 2019.

[57] T. Jonker, "The development of maintenance strategies for offshore wind farms," TUDelft, Delft, 2017.

[58] V. Yu, T. Huynh Anh Le, T.-S. Su and S.-W. Lin, "Optimal Maintenance Policy for Offshore Wind Systems," *Energies,* vol. 14, no. 19, 2021.

[59] GL Noble Denton, "GUIDELINES FOR MARINE TRANSPORTATIONS," Noble Denton Group Limited, 2010.

[60] A. Natskår, T. Moan and P. Ø. Alvær, "Uncertainty in forecasted environmental conditions for reliability analyses of marine operations," *Ocean Engineering,* vol. 108, pp. 636-647, 2015.

[61] National Weather Service, "Significant Wave Height," US Dept of Commerce, [Online]. Available: https://www.weather.gov/mfl/waves. [Accessed 25 September 2023].

[62] T. Gintautas, J. Dalsgaard Sørensen and S. Ringdalen Vatne, "Towards a Risk-based Decision Support for Offshore Wind Turbine Installation and Operation & Maintenance," *Energy Procedia,* vol. 94, pp. 207-217, 2016.

[63] DNV, "Marine Operations, General DNV-OS-H101," October 2011. [Online]. [Accessed 26 October 2023].

[64] E. Gaertner, J. Rinken, L. Sethuraman, F. Zahle, B. Anderson, G. Barter, N. Abbas, F. Meng, P. Bortolotti, W. Skrzypinski, G. Scott, R. Feil, H. Bredmose, K. Dykes, M. Shields, C. Allen and A. Viselli, "Definition of the IEA Wind 15-Megawatt Offshore Reference Wind Turbine," March 2020. [Online]. Available: https://www.nrel.gov/docs/fy20osti/75698.pdf. [Accessed 25 06 2023].

[65] A. M. R. Lourenço, "Advanced Operation and Maintenance Strategies Considering Turbine Interaction - Impact on Wind Farm Economics," Instituto Superior Técnico, Lisbon, 2023.

[66] "O.4.1 Crew transfer vessels," [Online]. Available: https://guidetofloatingoffshorewind.com/guide/o-operations-and-maintenance/o-4-offshore-vessels-and-logistics/o-4-1-crew-transfer-vessels/.

[67] WindPowerNL, "Damen's FCS 2710 one step closer to suit US offshore wind market," WindPowerNL, 12 October 2020. [Online]. Available: https://windpowernl.com/2020/10/12/damens-fcs-2710-one-step-closer-to-suit-us-offshore-wind-market/. [Accessed 15 August 2023].

[68] A. Cavalic, "Rapid developments in offshore market require new production methods for Fast Crew Suppliers," Offshore-Energy.biz, 31 May 2023. [Online]. Available: https://www.offshore-energy.biz/rapid-developments-in-offshore-market-require-new-production-methods-for-fast-crew-suppliers/. [Accessed 15 August 2023].

[69] D. Foxwell, "EnBW to test 'game-changing' crew transfer vessel on Baltic-1 and 2," Riviera Maritime Media, 17 May 2021. [Online]. Available: https://www.rivieramm.com/news-content-hub/news-content-hub/enbw-to-test-lsquogame-changingrsquo-crew-transfer-vessel-on-baltic-1-and-2-65511. [Accessed 15 August 2023].

[70] D. Foxwell, "New CTV is first designed and built in France," Riviera Maritime Magazine, 03 May 2022. [Online]. Available: https://www.rivieramm.com/news-content-hub/news-content-hub/new-ctv-is-first-designed-and-built-in-france-70906. [Accessed 15 August 2023].

[71] Anker, "Electricity Usage: How Much Energy Does an Average House Use," 02 June 2023. [Online]. Available: https://www.anker.com/blogs/home-power-backup/electricity-usage-how-much-energy-does-an-average-house-use. [Accessed 13 September 2023].

[72] E. Alaejos, "The momentum of offshore wind in Europe," Siemens Gamesa, 09 February 2021. [Online]. Available: https://www.siemensgamesa.com/explore/journal/2021/02/siemens-gamesa-wind-europe-report. [Accessed 14 September 2023].

[73] D. Bonvik-Stone, "Get the Alpha Factor: Waves, Work & Wider Weather Windows Offshore," Miros Group, 13 January 2021. [Online]. Available: https://www.miros-group.com/get-the-alpha-factor-waves-work-wider-weather-windows-offshore/. [Accessed 26 October 2023].

Appendix

Table A 1 - Results for Binary criterium with Regular CTV, using representative wind conditions

Year	Optimized Scheduling Energy Loss [MWh]	Sequential Scheduling Energy Loss [MWh]	Percentual Improvement with respect to Sequential Scheduling	Worst Scheduling Energy Loss [MWh]	Percentual Improvement with respect to Worst Scheduling
1992	4848.78	4998.10	2.99%	5318.67	8.83%
1993	2470.23	2612.78	5.46%	2877.80	14.16%
1994	5117.63	5461.02	6.29%	5648.38	9.40%
1995	4180.04	4496.27	7.03%	4710.40	11.26%
1996	2904.92	3147.93	7.72%	3378.83	14.03%
1997	3501.54	3664.46	4.45%	3914.04	10.54%
1998	3022.24	3237.38	6.65%	3383.41	10.67%
1999	3352.76	3568.53	6.05%	3909.92	14.25%
2000	3328.67	3643.82	8.65%	3826.59	13.01%
2001	3437.10	3660.53	6.10%	3831.07	10.28%
2002	5367.26	5583.25	3.87%	5842.48	8.13%
2003	3880.85	4026.66	3.62%	4276.12	9.24%
2004	2430.71	2563.76	5.19%	2756.54	11.82%
2005	2328.03	2544.97	8.52%	2826.07	17.62%
2006	2064.44	2159.06	4.38%	2277.30	9.35%
2007	2704.38	2840.02	4.78%	2952.99	8.42%
2008	2681.25	2872.68	6.66%	3073.03	12.75%
2009	2395.31	2554.36	6.23%	2758.27	13.16%
2010	4276.00	4511.98	5.23%	4800.55	10.93%
2011	2058.20	2166.44	5.00%	2328.49	11.61%
2012	2445.08	2576.71	5.11%	2762.17	11.48%
Total	68795.4	72890.7	5.62%	77453.1	11.18%
Average	3276.0	3471.0	5.62%	3688.2	11.18%

Table A 2 - Results for Binary criterium with Regular CTV, using hourly wind conditions

Year	Optimized Scheduling Energy Loss [MWh]	Sequential Scheduling Energy Loss [MWh]	Percentual Improvement with respect to Sequential Scheduling	Worst Scheduling Energy Loss [MWh]	Percentual Improvement with respect to Worst Scheduling
1992	4596.11	4715.61	2.53%	4912.46	6.44%
1993	2393.71	2451.20	2.35%	2570.11	6.86%
1994	4835.32	5142.56	5.97%	5163.52	6.36%
1995	3905.79	3998.88	2.33%	4214.54	7.33%
1996	2676.61	2772.81	3.47%	3028.14	11.61%
1997	3295.30	3363.24	2.02%	3476.85	5.22%
1998	2976.88	3098.86	3.94%	3092.77	3.75%
1999	3451.92	3597.82	4.06%	3800.95	9.18%
2000	3421.87	3579.11	4.39%	3645.61	6.14%
2001	3345.36	3456.46	3.21%	3479.53	3.86%
2002	4970.57	5044.55	1.47%	5291.21	6.06%
2003	3906.66	3894.84	-0.30%	4029.85	3.06%
2004	2601.24	2622.39	0.81%	2694.47	3.46%
2005	2527.84	2604.83	2.96%	2774.90	8.90%
2006	2089.13	2093.74	0.22%	2183.48	4.32%
2007	2786.45	2863.42	2.69%	2924.09	4.71%
2008	2870.49	3012.79	4.72%	3155.81	9.04%
2009	2809.94	2864.79	1.91%	2989.46	6.00%
2010	4493.23	4534.19	0.90%	4701.16	4.42%
2011	2126.34	2191.30	2.96%	2285.28	6.95%
2012	2302.36	2407.66	4.37%	2538.92	9.32%
Total	68383.1	70311.0	2.74%	72953.1	6.26%
Average	3256.3	3348.1	2.74%	3474.0	6.26%

Table A 3 - Results for Binary criterium, comparison between Novel CTVs and Regular CTVs

Year	Optimized Scheduling Energy Loss [MWh] with Novel CTVs	Optimized Scheduling Energy Loss [MWh] with Regular CTVs	Sequential Scheduling Energy Loss [MWh] with Novel CTVs	Sequential Scheduling Energy Loss [MWh] with Regular CTVs
1992	6160.76	4596.11	4715.61	5133.43
1993	2635.48	2393.71	2451.20	2546.76
1994	6069.81	4835.32	5142.56	5068.75
1995	4127.98	3905.79	3998.88	3998.88
1996	3208.07	2676.61	2772.81	3307.18
1997	2763.77	3295.30	3363.24	3512.26
1998	5275.60	2976.88	3098.86	3576.32
1999	6527.41	3451.92	3597.82	3821.73
2000	3793.16	3421.87	3579.11	3477.99
2001	4645.70	3345.36	3456.46	3622.89
2002	7290.73	4970.57	5044.55	5709.83
2003	4685.00	3906.66	3894.84	4031.74
2004	3033.42	2601.24	2622.39	2611.84
2005	4920.30	2527.84	2604.83	2678.64
2006	3184.40	2089.13	2093.74	2212.73
2007	2583.96	2786.45	2863.42	2905.22
2008	2600.21	2870.49	3012.79	3012.79
2009	3680.49	2809.94	2864.79	3144.87
2010	5363.36	4493.23	4534.19	4692.60
2011	5886.75	2126.34	2191.30	3205.43
2012	5844.86	2302.36	2407.66	2841.15
Total	94281.2	68383.1	70311.0	75113.0
Average	4489.58	3256.34	3348.14	3576.81

Table A 4 - Results for Non-Binary Criterium

Year	Sequential Scheduling Energy Loss [MWh] with Novel CTVs and Non-Binary Crtierium, 5T	Optimized Scheduling Energy Loss [MWh] with Novel CTVs and Non-Binary Crtierium, 5T	Optimized Scheduling Energy Loss [MWh] with Novel CTVs and Non-Binary Crtierium, 6T
1992	1810.313107	1815.303346	1493.837295
1993	877.4896301	860.4837245	407.7903681
1994	1956.176051	1955.899785	1418.813854
1995	518.0638831	516.9859498	166.0398184
1996	1056.163781	1010.337554	687.8748915
1997	1891.868981	1763.095711	1478.269541
1998	2473.15437	2424.434442	2081.282011
1999	2544.294197	2416.759043	2103.906044
2000	2726.435313	2592.518539	2267.717202
2001	2633.883909	2627.650641	2466.885205
2002	3381.634696	3330.370704	2942.048741
2003	2925.601157	2820.693961	2367.96907
2004	1862.545774	1774.088681	1289.88899
2005	1395.454786	1392.419928	1111.770261
2006	1571.021709	1535.62886	1161.556151
2007	1883.09042	1830.872655	1467.891806
2008	1803.86946	1739.621811	1404.074746
2009	2956.093525	2812.565204	2609.879453
2010	3067.192917	3074.378378	2227.332468
2011	2789.383493	2775.110148	2337.752671
2012	3646.632683	3556.359855	2945.970532
Total	45770.36384	44625.57892	36438.55112
Average	2179.541135	2125.027568	1735.169101